Next, an IR measurement was performed to directly detect the succinimide structure in the condition where PBLA reacted with 0.005-fold DIP in DMSO at 35 °C for 30 min. In the IR spectrum of the product, the amide I, amide II and ester peaks almost disappeared and the imide peaks of the succinimidyl ring appeared clearly at 1717 cm^{-1} and 1800 cm^{-1}, as shown in Fig. 4A and B. The IR spectrum of the product was very similar to that of the model imide, *N*-ethyl-succinimide (data not shown) and similar to the spectrum of Poly(succinimide) which has been reported [46]. Therefore, it is reasonable to conclude that DIP catalytically transduces the BLA residue to succinimide, an active intermediate, which then quantitatively converted to aspartamide, and that aspartamide includes β-isomer.

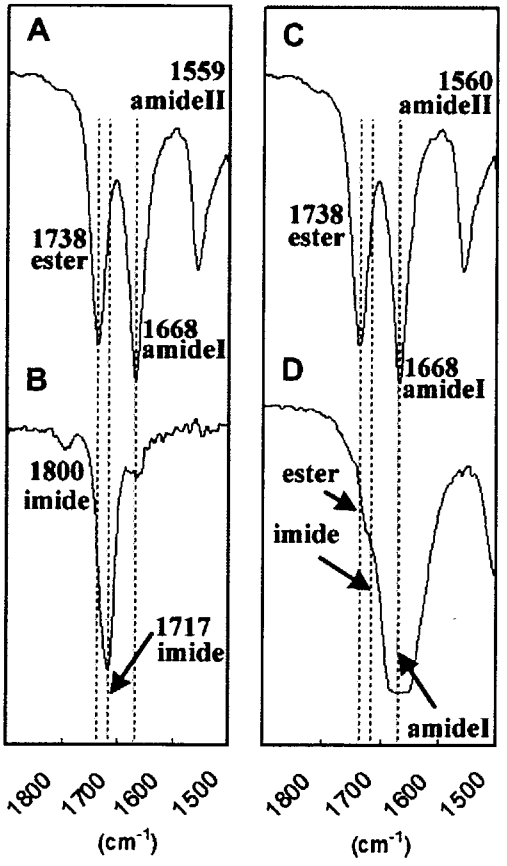

Fig. 4. Infrared absorption spectra with assignments at a range of 1800–1500 cm^{-1} of (A) PBLA, (B) PBLA reacting with 0.005-fold DIP in DMSO for 30 min, (C) PBLA reacting with 0.005-fold DIP in CH_2Cl_2 for 24 h, and (D) PBLA reacting with 1-fold TEA in CH_2Cl_2 for 12 h.

3.3.2. Identification of intermediate structure and kinetics in CH_2Cl_2

Similarly, the identification of an intermediate structure in CH_2Cl_2 was carried out to explore the mechanism involved in the quantitative aminolysis reaction in apolar solvents. The ^1H NMR spectra were obtained in the condition where PBLA reacted with 0.5-fold DIP in CD_2Cl_2 at 35 °C as shown in Fig. 5. The sharp peak of CH_2 (f) of the leaving benzyl alcohol appeared at 4.6 ppm with a gradual increase in the intensity, with the reaction time occurring more slowly than that in the DMSO-d_6 system. Eventually, 47% of benzyl alcohol was eliminated in 237 h. Nevertheless, no peak corresponding to succinimide as an intermediate structure was found in the spectra from (A) to (E), unlike in the DMSO-d_6 system. An IR measurement was carried out in the condition where PBLA reacted with the catalytic amount of DIP for 24 h in CH_2Cl_2. The spectrum obtained after 24 h was quite similar to that of PBLA (Fig. 4C) without any sign of succinimide ring formation. Further analysis was then carried out using triethylamine (TEA) as a weak base, which can act as a catalyst leading to formation of the succinimide ring, yet cannot undergo an aminolysis reaction because of the lack of a primary amino group. Eventually, the solution of PBLA reacting with an equivalent TEA for 24 h became turbid, and its IR spectrum clearly included the band assignable to the imide structure (Fig. 4D), indicating the formation of a succinimide structure.

Note that poly(succinimide) is known to be insoluble in CH_2Cl_2 [46], being consistent with the precipitate formation in the reaction mixture of PBLA with TEA in CH_2Cl_2. In the reaction system with DIP, the produced succinimide moiety promptly reacted with the primary amino group of DIP to form an aspartamide with a flanking diisopropylaminoethyl group because the succinimidyl ring formation was the rate-limiting step ($k_1 < k_3$), eventually maintaining the polymer solubility in CH_2Cl_2.

3.4. Stereoselectivity

A measurement of the specific optical rotation was conducted to analyze the racemization and conformational change of the polymer strand during the aminolysis of PBLA. Notably, a significant difference in $[\alpha]_D$ was observed between the polymers dissolved in DMSO and CH_2Cl_2 (Fig. 6). $[\alpha]_D$ of the polymer in DMSO immediately became almost

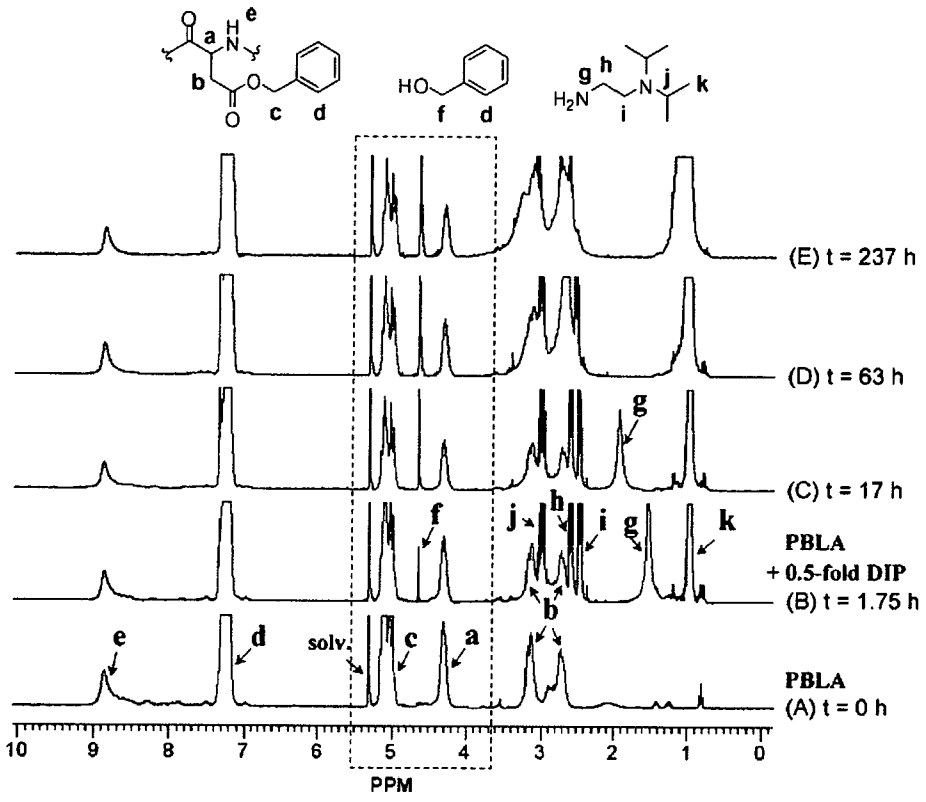

Fig. 5. Time-trace of ^{1}H NMR spectra of PBLA reacting with 0.5-fold DIP in CD_2Cl_2 at 35 °C.

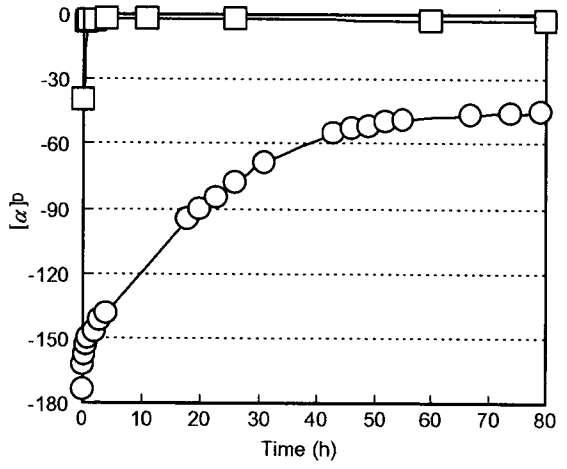

Fig. 6. Time-trace of $[\alpha]_D$ of PBLA reacting with 1-fold DIP at room temperature in DMSO (□) and CH_2Cl_2 (○).

zero after the DIP addition, suggesting the prompt racemization. $[\alpha]_D$ of PBLA in CH_2Cl_2 showed a highly negative value compared to that in DMSO due to the formation of the left-handed α-helix. Then, after the addition of DIP, alternatively, $[\alpha]_D$ of the system revealed a gradual shift in the positive direction and converged from the value of −180 to −45 after 80 h. It should be noted that the $[\alpha]_D$ value of −45 coincided with that for the random coiled PBLA in polar solvents such as DMSO.

Further analysis revealed that racemization occurred in the polar solvents and was effectively prohibited in the apolar solvents (Table 1), indicating that the $k_{2\_apolar\ solvent}$ was quite smaller than the $k_{2\_polar\ solvent}$. It is worth mentioning that the optical purity of the L-isomers was maintained with the yield of 95% in CH_2Cl_2, which is unprecedentedly high.

Racemization occurs by the rearrangement of the eliminated proton in the α position from Si face known as the keto–enol tautomerization (Scheme 2). It is reasonable to assume that the keto–enol tautomerzation is thermodynamically easy to occur in the polar solvents and not in the apolar solvents. Therefore, the racemization was effectively prohibited in the apolar solvents. Furthermore, the secondary structure of the polymer strands may also be a factor affecting racemization. The formation of an enol structure may be restricted in the α-helical structure because of the

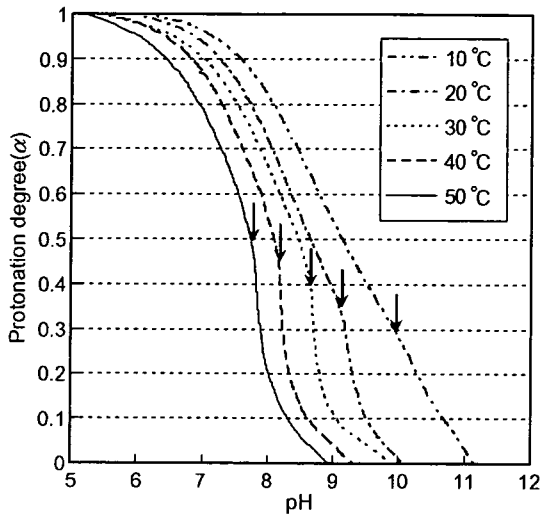

Fig. 7. Protonation degree (α) as a function of pH (α/pH curve) for PAsp(DIP) prepared in DMF. Each arrow in the figure indicates the pH at which the transmittance of the polymer solution decreased to 95%.

intramolecular hydrogen bond. However, further analyses may be needed to clearly explain the reaction scheme.

3.5. Solution properties of PAsp(DIP)

The analysis of the aqueous solution property of PAsp(DIP) synthesized in DMF was performed by the potentiometric titration and transmittance measurement to obtain α–pH curves at various temperatures (Fig. 7). The transmittance sharply decreased at a specific pH for all of the measuring temperatures, suggesting that the polymer became hydrophobic with the deprotonation to precipitate out of the solution.

The apparent pK_a ($pK_{a,app}$) values defined as a pH of $\alpha = 0.5$ increased with the decrease of the temperature from $pK_{a,app} = 7.7$ at 50 °C to $pK_{a,app} = 9.3$ at 10 °C. These results indicate that at a higher temperature, PAsp(DIP) is more liable to release proton because it is energetically preferable for the amphiphilic polycations to release highly condensed protons on the polymer strand to form the collapsed globule. However, stabilization due to the hydrophobic hydration was promoted at a lower temperature to maintain the solubility of PAsp(DIP) even at the higher range of pH. Eventually, PAsp(DIP) will be feasible to use as a novel smart materials with dual sensitivity i.e., sensitivity to both pH and temperature.

4. Conclusion

It was revealed that the aminolysis of PBLA, which proceeds involving a succinimide intermediate, was useful for quantitatively introducing the functional group into the side chain of PBLA. Moreover, racemization was effectively suppressed through the aminolysis in CH_2Cl_2 to give polyaspartamide with an appreciably high optical purity of 95%. This optical purity will apparently be a great advantage in its application as biomaterials. The cationic PAsp(DIP) synthesized by this method showed the dual sensitivity to pH and temperature, and thus may have a potential utility as novel smart biomaterials. In conclusion, this method of aminolysis is a simple and efficient way of constructing a polyaspartamide library from PBLA as a single platform polymer, and can be applied for screening the various utilities of structurally well-defined polyaspartamide derivatives as functionality materials.

Acknowledgements

The authors wish to express their gratitude to Prof. T. Tsuruta, Professor Emeritus, The University of Tokyo, for his valuable discussions and critical comments on this research. This work was financially supported by the Core Research for Evolutional Science and Technology (CREST) from the Japan Science and Technology Agency (JST).

References

[1] S. Jean-Claude, B. Jean-Claude, React. Polym. 12 (1990) 3.
[2] S. Jean-Claude, B. Jean-Claude, React. Polym. 12 (1990) 133.
[3] S. Jean-Claude, B. Jean-Claude, React. Polym. 13 (1990) 1.
[4] R. Arshdy, Adv. Polym. Sci. 111 (1994) 1.
[5] H. Mao, C. Li, Y. Zhang, S. Furyk, P.S. Cremer, D.E. Bergbreiter, Macromolecules 37 (2004) 1031.
[6] A. Godwin, M. Hartenstein, A.H.E. Müller, S. Brocchini, Angew. Chem. Int. Ed. 40 (2001) 594.
[7] W. Wu, B. Jin, G. Krippner, K. Watson, Bioorg. Med. Chem. Lett. 10 (2000) 341.
[8] L.E. Strong, L.L. Kiessling, J. Am. Chem. Soc. 121 (1999) 6193.
[9] A. Carrillo, K. Gujraty, P. Rai, R. Kane, Nanotechnology 16 (2005) S416.
[10] P. Strohriegl, Makromol. Chem. 194 (1993) 363.
[11] Y.S. Yang, G.R. Qi, J.W. Qian, S.L. Yang, J. Appl. Polym. Sci. 68 (1998) 665.
[12] Y.X. Liu, Z.J. Du, Y. Li, C. Zhang, C.J. Li, X.P. Yang, H.Q. Li, J. Appl. Polym. Sci. 44 (2006) 6880.
[13] R. Luxenhofer, R. Jordan, Macromolecules 39 (2006) 3509.

[14] B. Parrish, R.B. Breitenkamp, T. Emrick, J. Am. Chem. Soc. 127 (2005) 7404.
[15] T.J. Deming, Adv. Drug. Deliv. Rev. 54 (2002) 1145.
[16] S. Brocchini, Adv. Drug. Deliv. Rev. 53 (2001) 123.
[17] M. Ali, S. Brocchini, Adv. Drug. Deliv. Rev. 58 (2006) 1671.
[18] A. Lavasanifar, J. Samuel, G.S. Kwon, Adv. Drug. Deliv. Rev. 54 (2007) 169.
[19] G. Pratesi, G. Savi, G. Pezzoni, O. Bellini, S. Penco, S. Tinelli, F. Zunino, Brit. J. Cancer 52 (1985) 841.
[20] H.J.-P. Ryser, W.-C. Shen, Proc. Natl. Acad. Sci. USA 75 (1978) 3867.
[21] G.Y. Wu, C.H. Wu, J. Biol. Chem. 262 (1987) 4429.
[22] N. Lupu-Lotan, A. Yaron, A. Berger, M. Sela, Biopolymers 3 (1965) 625.
[23] A.D. Marre, H. Soyez, E. Schacht, J. Pytela, Polymer 35 (1994) 2443.
[24] M.G. Meirim, E.W. Neuse, F. Parisi, Angew. Makromol. Chem. 175 (1990) 141.
[25] E.W. Neuse, A.G. Perlwitz, S. Schmitt, Angew. Makromol. Chem. 181 (1990) 153.
[26] E.W. Neuse, A.G. Perlwitz, S. Schmitt, Angew. Makromol. Chem. 192 (1991) 35.
[27] E.W. Neuse, B.B. Patel, C.W.N. Mbonyana, J. Inorg. Organomet. Polym. 1 (1991) 147.
[28] J.C. Swarts, E.W. Neuse, G.J. Lamprecht, J. Inorg. Organomet. Polym. 4 (1994) 143.
[29] R.W. Niven, F. Rypacek, P.R. Byron, Pharm. Res. 7 (1990) 990.
[30] M. Schwamborn, Polym. Degrad. Stab. 59 (1998) 39.
[31] K.C. Low, A.P. Wheeler, L.P. Koskan, Adv. Chem. Ser. 248 (1996) 99.
[32] T. Nakato, M. Yoshitake, K. Matsubara, M. Tomida, T. Kakuchi, Macromolecules 31 (1998) 2107.
[33] S.K. Wolk, G. Swift, H.-P. Yi, K.M. Yocom, R.L. Smith, E.S. Simon, Macromolecules 27 (1994) 7613.
[34] K. Itaka, N. Kanayama, N. Nishiyama, W.-D. Jang, Y. Yamasaki, K. Nakamura, H. Kawaguchi, K. Kataoka, J. Am. Chem. Soc. 126 (2004) 13612.
[35] S. Fukushima, K. Miyata, N. Nishiyama, N. Kanayama, Y. Yamasaki, K. Kataoka, J. Am. Chem. Soc. 127 (2005) 2810.
[36] Y. Bae, W.-D. Jang, N. Nishiyama, S. Fukushima, K. Kataoka, Mol. Biosyst. 1 (2005) 242.
[37] A. Koide, A. Kishimura, K. Osada, W.-D. Jang, Y. Yamasaki, K. Kataoka, J. Am. Chem. Soc. 128 (2006) 5988.
[38] N. Kanayama, S. Fukushima, N. Nishiyama, K. Itaka, W.-D. Jang, K. Miyata, Y. Yamasaki, U.-I. Chung, K. Kataoka, Chem. Med. Chem. 1 (2006) 439.
[39] Arnida, N. Nishiyama, N. Kanayama, W.-D. Jang, Y. Yamasaki, K. Kataoka, J. Control. Release 115 (2006) 208.
[40] H.G. Schild, Prog. Polym. Sci. 17 (1992) 163.
[41] D.D. Perrin, W.L.F. Armarego, D.R. Perrin, Purification of Laboratory Chemicals, Pergamon, Oxford, 1980.
[42] K. Nokihara, J. Gerhardt, Chirarity 13 (2001) 431.
[43] P. Dubin, F.E. Karasz, Biopolymer 11 (1972) 1745.
[44] R.H. Karlson, K.S. Norland, G.D. Fasman, E.R. Blout, J. Am. Chem. Soc. 82 (1960) 2268.
[45] E.R. Blout, Biopolymers Symp. 1 (1964) 397.
[46] A.J. Adler, G.D. Fasman, E.R. Blout, J. Am. Chem. Soc. 85 (1963) 90.
[47] C.G. Swain, J.F. Brown, J. Am. Chem. Soc. 74 (1952) 2538.
[48] J.L. Radkiewicz, H. Zipse, S. Clarke, K.N. Houk, J. Am. Chem. Soc. 118 (1996) 9148.
[49] G.G. Smith, G.V. Reddy, J. Org. Chem. 54 (1989) 4529.
[50] T. Takata, T. Shimo-Oka, K. Miki, N. Fujii, Biochem. Biophys. Res. Commun. 334 (2005) 1022.
[51] N. Fujii, K. Harada, Y. Momose, N. Ishii, M. Akaboshi, Biochem. Biophys. Res. Commun. 263 (1999) 322.
[52] N. Fujii, L.J. Takemoto, Y. Momose, S. Matsumoto, K. Hiroki, M. Akaboshi, Biochem. Biophys. Res. Commun. 265 (1999) 746.
[53] A.C.T. Van Duin, M.J. Collins, Org. Geochem. 29 (1998) 1227.
[54] T. Nakato, A. Kusuno, T. Kakuchi, J. Polym. Sci. Part A: Polym. Chem. 38 (2000) 117.

DOI: 10.1002/cmdc.200700093

pH-Responsive Multi-PEGylated Dual Cationic Nanoparticles Enable Charge Modulations for Safe Gene Delivery

May P. Xiong,[a] Younsoo Bae,[b] Shigeto Fukushima,[c] M. Laird Forrest,[a] Nobuhiro Nishiyama,[b] Kazunori Kataoka,*[b, c] and Glen S. Kwon*[a]

In gene therapy, the cytotoxicity of many polycations is undesirable and has been attributed to nonspecific membrane destabilizing effects and intracellular polyplex-mediated toxicity. To help prolong the pharmacokinetic profile of nonviral vehicles for gene delivery, the cationic surface charge of current systems is typically shielded through the conjugation of polyethylene glycol (PEG) chains to the particle surface. However, the design of an intelligent polycation with environment-sensing charge modulations is essential to minimize cytotoxicity and enhance gene expression. We have designed a novel di-cationic block copolymer, poly(aspartate-hydrazide)-block-poly(L-lysine), capable of pH-mediated endosomal membrane disruption based on charge interactions, which has negligible toxicity elsewhere to the cell. The poly(L-lysine) segment, with a high pK_a value of ~9.4, preferentially forms a poly-ion complex with the negative phosphate groups of pDNA, whereas the pH-responsive poly(aspartate-hydrazide) segment, with the comparatively lower pK_a ~5.0, is characterized by a substantial fraction of unprotonated amino groups at physiological pH. As a consequence, complexation between such a polymer and pDNA leads to the formation of a two-layered nanoparticle. In particular, the nanoparticle possesses an unprotonated pH-responsive segment to serve as both a scaffold for acid-labile linkages of various moieties such as aldehyde-PEG and to transition from neutral to charged for disrupting endosomal membranes, and safely enhancing gene expression. Our system supports an endosomal escape mechanism based on charge interactions rather than the proton-sponge effect, and may be an important step towards engineering new classes of intelligent nonviral vectors.

Introduction

Intelligent biomaterials that can emulate natural viruses by adapting to their environment with minimal toxicity to the cell are highly desired for gene therapy. These synthetic vehicles are often internalized in many different cell lines through receptor-mediated endocytosis into clathrin-coated vesicles that fuse to form early endosomes (pH 7.4–6), which become late endosomes (pH 6.0–5.5), and eventually lysosomes (pH 5.0).[1–3] Research to date has primarily emphasized gene delivery carriers equipped with endosomal buffering, also known as the proton sponge effect (PSE),[4] to escape acidic endolysosomes for mediating gene expression.[5,6] However, natural viruses are not equipped with endosomal buffering properties. Instead, they frequently exploit the decrease in pH to expose fusogenic domains that can disrupt the endosomal or lysosomal membrane, resulting in release of the virus into the cytoplasm. Similarly, endosomal membrane disruptions with charged surfaces may also play an important role in helping particles escape from endosomes.[7,8] Despite their positive attributes, many common polycations are cytotoxic due to nonspecific membrane destabilizing effects and intracellular polyplex-mediated toxicity.[9–12] From these observations, we have postulated that the appreciable effect of charge interaction on endosomal escape might be observed even in the absence of the PSE by designing a pH-responsive polycation with dual functional pK_a values (high and low) to emulate the escape mechanism used by natural viruses.

[a] Dr. M. P. Xiong, Dr. M. L. Forrest, Prof. G. S. Kwon
Division of Pharmaceutical Sciences
School of Pharmacy, University of Wisconsin
777 Highland Avenue, Madison, WI 53705-2222 (USA)
Fax: (+1) 608-262-5345
E-mail: gskwon@pharmacy.wisc.edu

[b] Dr. Y. Bae, Dr. N. Nishiyama, Prof. K. Kataoka
Center for Disease Biology and Integrative Medicine
Graduate School of Medicine, The University of Tokyo
7-3-1 Hongo, Bunkyo-ku, Tokyo 113-0033 (Japan)
and
Center for NanoBio Integration, The University of Tokyo
7-3-1 Hongo, Bunkyo-ku, Tokyo 113-8656 (Japan)
Fax: (+81) 3-5841-7139
E-mail: kataoka@bmw.t.u-tokyo.ac.jp

[c] Dr. S. Fukushima, Prof. K. Kataoka
Department of Materials Engineering
Graduate School of Engineering, The University of Tokyo
7-3-1 Hongo, Bunkyo-ku, Tokyo 113-8656 (Japan)

Supporting information for this article is available on the WWW under http://www.chemmedchem.org or from the author.

Results and Discussion

Chemical synthesis

Figure 1 shows the chemical structure of the dual-cationic block copolymer, poly(aspartate-hydrazide)-*block*-poly(L-lysine) (abbreviated BC), based on functional pK_a differences between respective cationic blocks. The poly(L-Lys) (PLL) segment, with a high pK_a value of ~9.4, preferentially forms a poly-ion complex (PIC) with the negative phosphate groups of pDNA, whereas the pH-responsive poly(Asp-Hyd) segment, with a comparatively lower pK_a value of ~5.0, is characterized by a substantial fraction of unprotonated amino groups at physiological pH (Figure 1a). Some of these Asp-Hyd residues are coupled to aldehyde-PEG chains (ALD-PEG) through acid-labile hydrazone linkages to impart favorable stealth properties to the PIC (Figure 1b). As a consequence, the complexation between such a polymer and pDNA may lead to the formation of a two-layered particle possessing an unprotonated pH-responsive poly(Asp-Hyd) segment that functions as both a scaffold for acid-labile linkages of various moieties, and that has the ability to undergo a transition from neutral to charged for disrupting endosomal membranes, as illustrated in Figure 2. Therefore, the PIC described herein is formed from associations of such block copolymer chains: a) a pDNA condensing core made of PLL chains (known for not contributing to the PSE), and b) a shell composed of segments with repeating Asp-Hyd residues.

The backbone of the block copolymer is derived from poly(β-benzyl-L-aspartate)-*block*-poly(L-lysine) (PBLA-*b*-PLL; see Supporting Information). PBLA was prepared by the ring-opening polymerization of β-benzyl-L-aspartate *N*-carboxyanhydride (BLA-NCA), initiated by the terminal $-NH_2$ group of butylamine to yield a polymer with narrow distribution and degree of polymerization (DP) of 36 (Figure 1S). The terminal amine on PBLA was used to initiate ring-opening polymerization of lysine(TFA) *N*-carboxyanhydride monomers (Lys-NCA) to yield PBLA-*b*-PLL(TFA) with DP = 53, in accordance with previous work in which a PLL length of ~50 was determined optimal for gene expression (Figure 2S).[5,13] Next, hydrazide groups were conjugated with a substitution efficiency near 100 mol% on PBLA, using a procedure reported by Bae et al.,[14,15] to give poly(Asp-Hyd)-*b*-PLL(TFA) (TFA = trifluoroacetyl). When deprotected, this polymer yields BC. Finally, ALD-PEG (M_W = 7000 g mol^{-1}) was synthesized following procedures reported by Nagasaki et al.[16] and characterized with ^{1}H NMR ($CDCl_3$; determined 91% acetal conversion into aldehyde groups) and gel permeation chromatography (GPC) (TSK-gel G3000PWXL and TSK-gel G4000PWXL; 10 mM LiCl in *N*,*N*-dimethylformamide (DMF); 0.8 mL min^{-1}; polydispersity index (PDI): 1.03). The final PEGylated block copolymers [poly(Asp-Hyd-PEG)-*b*-PLL] had either five ALD-PEG chains conjugated to each poly(Asp-Hyd) block to form the acid-labile hydrazone linkage (pH-PBC), or six COOH-PEG chains conjugated covalently by amide linkages to hydrazide groups to generate the non-hydrolysable control (cov-PBC), as shown in Figures 3S and 4S. There are substantial unconjugated hydrazide groups that remain on each block copolymer chain.

Physical characterization

The protonation profile of BC reveals that hydrazide groups do not significantly buffer in the critical range known to be essential for PSE-mediated escape of endosomes (pH 5.0–6.0), similar

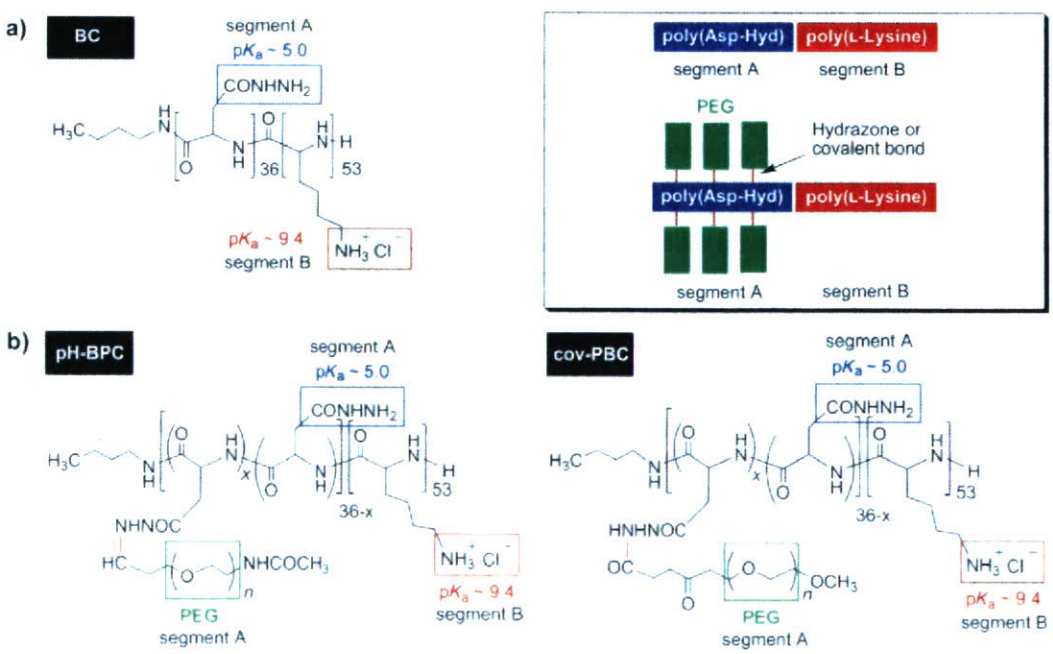

Figure 1. Structure of the block copolymers: a) poly(aspartate-hydrazide)-*block*-poly(L-lysine) (BC); b) pH-sensitive poly(aspartate-hydrazide-PEG)-*block*-poly(L-lysine) (pH-PBC), and covalent poly(aspartate-hydrazide-PEG)-*block*-poly(L-lysine) (cov-PBC). (See Supporting Information for synthesis.)

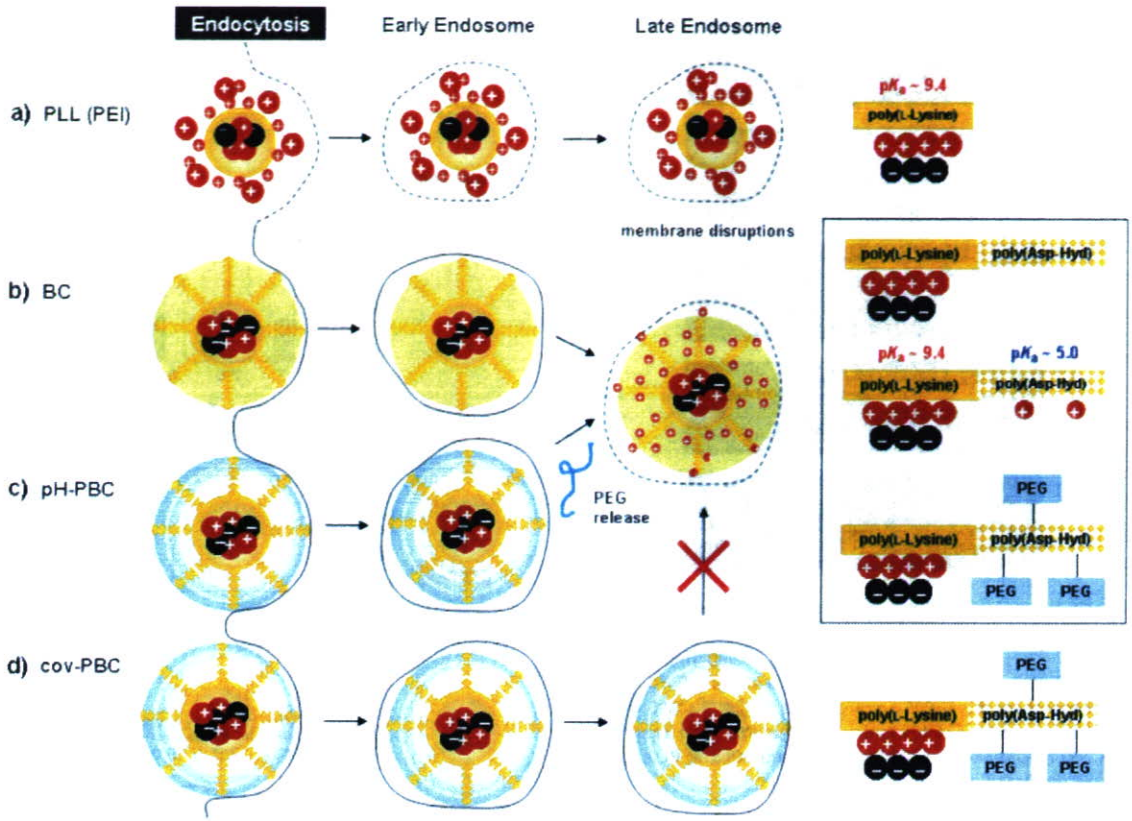

Figure 2. a) Cationic polyplexes formed with PLL (or PEI) are cytotoxic to cells. In contrast, neutral shielded particles [parts b), c), and d)] cause minimal membrane damage during endocytosis: Following a decrease in pH, hydrazide amino groups protonate (b) and/or acid-labile PEG chains are released (c). This increases endosomal membrane disturbances with the resulting charged particle and enhances escape into the cytosol (pH 7.4), whereupon sensing the new pH, hydrazide amino groups deprotonate again, once more imparting neutral properties to the PIC and minimizing intracellular toxicity. d) cov-PBC particles cannot release PEG chains following a decrease in pH, and this may minimize particle interactions with the endosomal membrane.

to PLL (Figure 3), and furthermore do not contribute significantly to pGL3 condensation at physiological pH, because mostly PLL groups undergo electrostatic interactions with pDNA (Figure 4). This suggests that the PIC formed is composed of a PLL–DNA core with poly(Asp-Hyd) segments on the surface. The effect of pH on colloidal properties of the PIC was also investigated (Figure 5). At pH 7.4, PICs formed with BC have mostly unprotonated hydrazide groups exposed on the surface (~5.0 mV), and counterion screening causes particles to exhibit aggregation behavior (diameter ~440 nm). However, as hydrazide groups on PICs become protonated with decreasing pH, charged cationic surfaces are generated (~35 mV), overcoming van der Waals interactions and resulting in electrostatic repulsions between individual particles (~100 nm). For pH-PBC, the size and ζ profiles are more informative than the averages reported (Figure 5, insert). Although average $\zeta < 8$ mV and average diameter is < 100 nm over the range of pH, the system is represented by distinct multimodal populations, indi-

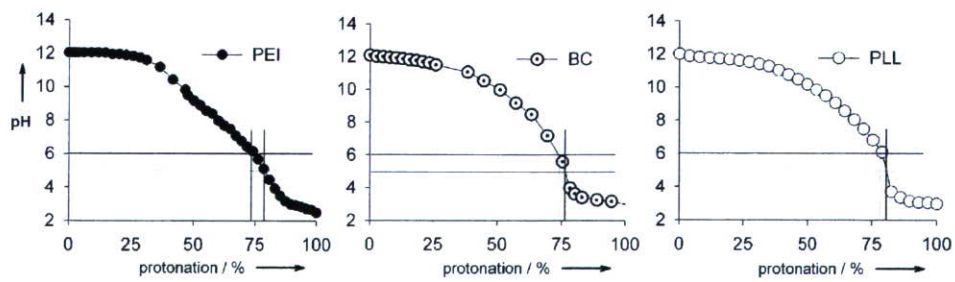

Figure 3. Protonation profiles comparing branched PEI, BC, and PLL. As expected, PEI can buffer over a relatively wide pH range. BC carries little buffering capacity, similar to PLL (note: error bars omitted to simplify profile). Table 1S summarizes the mol% of various amines on each polymer; only side chain terminal amines are considered. The data indicate that the presence of hydrazide groups on BC does not contribute significantly to endosomal buffering in the critical range of pH 5.0–6.0 essential to the PSE.

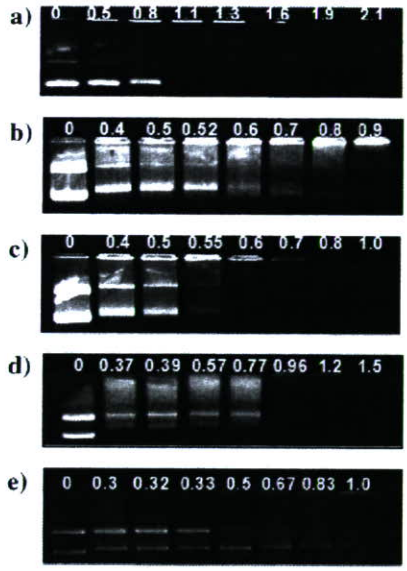

Figure 4. Isoelectric points (pI) of the polymer in complex with 1 μg pGL3; values indicate equivalent N/P ratios: a) PEI (25 000 g mol^{-1}), pI (*w/w*) = 0.20 μg, N/P = 1.1; b) BC (poly(Asp-Hyd)$_{36}$-PLL$_{49}$) (11 000 g mol^{-1}), pI (*w/w*) = 0.65 μg, N/P = 0.9; c) PLL$_{44}$ (9200 g mol^{-1}), pI = 0.40 μg, N/P = 0.7; d) pH-PBC (five PEG chains per BC, 46 000 g mol^{-1}), pI = 2.5 μg, N/P = 0.96; e) cov-PBC (six PEG chains per BC, 53 000 g mol^{-1}), pI = 4 μg, N/P = 1.0. Electrostatic interactions occur mostly between lysine groups and pGL3, as BC and PBC polymers have similar N/P ratios of ~1.

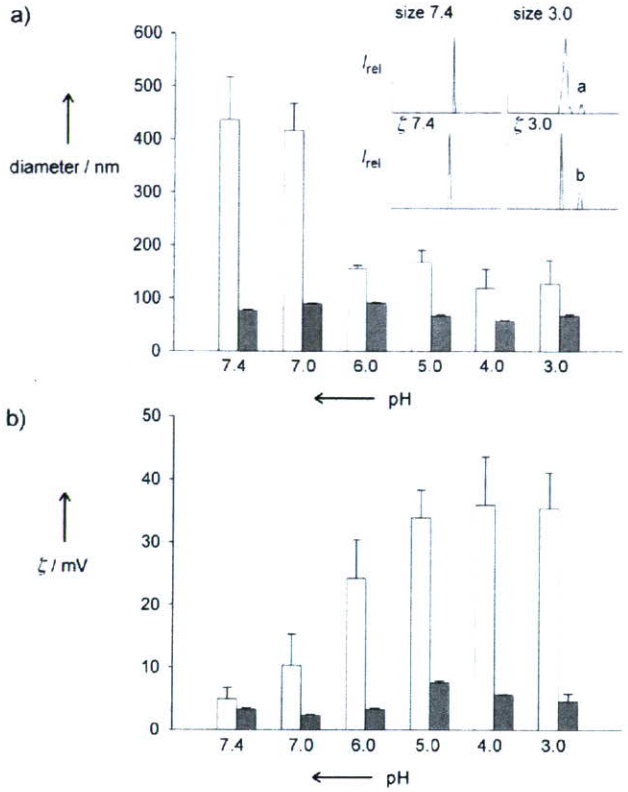

Figure 5. a) Size and b) ζ profiles for BC (white) and pH-PBC (gray) at the indicated pH values. Particles were formed at N/P = 20 (to concur with the transfection experiments) with 2 μg pGL3 in water, incubated for at least 30 min, and diluted with low-ionic-strength buffers of appropriate pH before size measurement. The same sample was then injected into the instrument to obtain ζ potentials. At pH 7.4, BC particles are ~440 nm with ζ potentials of ~5 mV. At pH 3.0, BC particles are ~100 nm with ζ potentials of ~35 mV. For pH-PBC, the particles are ~80 nm in diameter with a ζ value of ~3 mV at pH 7.4. At pH 3.0, the average size is ~70 nm and ζ ~5 mV. However, pH-PBC profiles under acidic conditions (insert) point to particle instability as PEG is released. Large aggregates (peak a) with higher ζ values (peak b) appear (multimodal populations were observed for all acidic pH values). In contrast, cov-PBC had single population profiles (data not shown). (Note: the values reported were calculated by averaging the sums of peak intensities multiplied by magnitudes.)

cative of reversible PEG release. This is in sharp contrast to the single population observed with cov-PBC under acidic conditions (data not shown). pH-Release studies confirm that, in a closed system, the hydrazone linkage is reversible and exhibits equilibrium behavior at various pH values over prolonged incubation (Figure 6).

Biological characterization

In addition, subsequent lactate dehydrogenase (LDH) release studies show that our dual-cationic polymer does not cause membrane toxicity when complexed with pDNA. At physiological pH, free PEI, PLL, and BC polymer chains have cationic properties that cause high levels of membrane toxicity to cells, relative to PEG-shielded polymers (Figure 7a,c). However, if BC (20 μg mL^{-1}) is complexed with pGL3, the presence of many unprotonated hydrazides on the surface of the PIC causes negligible membrane toxicity (Figure 7b). As BC concentration is increased in the presence of pGL3 (40 μg mL^{-1}), LDH release also increases, but that is most likely due to the presence of excess free polymers in solution with respect to pDNA concentration (Figure 7d). Our results imply that freely accessible charged polymers cause membrane-associated toxicity, but that membrane damage is minimized when the cationic PLL block is concealed within the PIC core.

We next compared the metabolic activity of our polymers both in free form and in complex with pGL3 to investigate the potential intracellular toxicity often associated with cationic polyplex-mediated uptake.[12] The free polymers (PEI and BC) with accessible cationic components caused greater metabolic toxicity to the cell following internalization (Figure 8a). PEG-shielded polymers exhibited low metabolic toxicity. On the other hand, PICs with concealed cationic PLL cores (BC, pH-PBC, and cov-PBC) gave little evidence of metabolic toxicity to the cell, in contrast to PEI-formulated particles (Figure 8b). These results correspond well with the LDH assay data.

Finally, we looked at the transfection efficiency of these polymers in five very different cell lines and found that pH-PBC and BC (both nontoxic) consistently resulted in higher gene expression relative to cov-PBC (Figure 9) and PLL (data not shown). Note that the trend in transfection between the polymers and across different cell lines is not consistent. This might be a result of the fact that in the absence of targeting ligands, various cell lines use different modes of particle internalization (such as clathrin and/or caveolae-mediated processes) that can ultimately affect uptake pathways and particle fate within the cell.[17–19] Importantly, however, there is a consistent

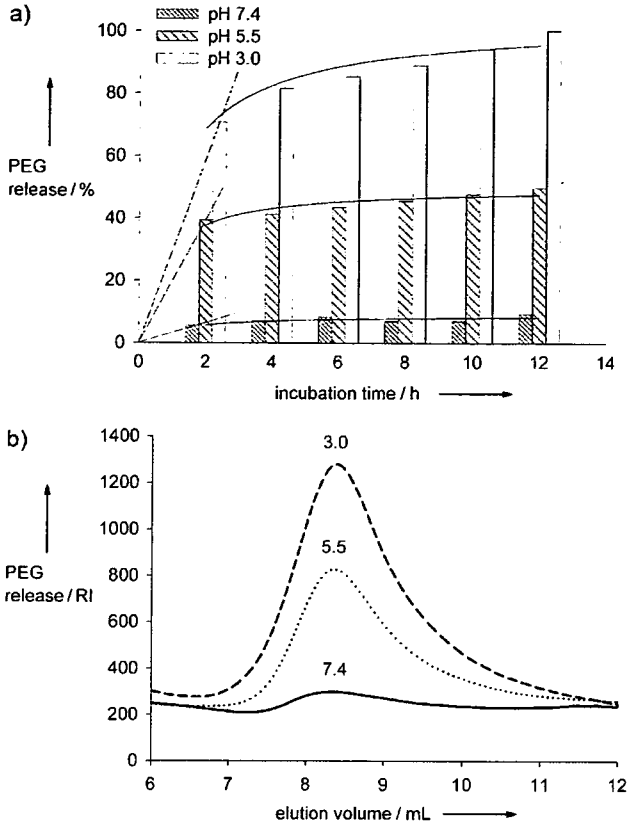

Figure 6. PEG release monitored by GPC: pH-PBC was injected into an OHpak SB-806M GPC column (injection volume: 20 μL; polymer: 2 mg mL^{-1}; of HEPES eluent: 10 mM, pH 7.4, 0.75 mL min^{-1}, 30 °C; Shodex, Kawasaki, Japan), and PEG release was detected by refractive index (RI) for 12 h. a) PEG falls off upon incubation at pH < 7.0, but the hydrazone bond is relatively stable at pH 7.4, with less than 10% PEG released over 12 h. The reversible nature of the hydrazone bond leads to an equilibrium state in the release profiles at different pH's. b) Sample curves at $t = 2$ h are shown with pH values indicated.

enhancement in gene expression for BC and pH-PBC compared with cov-PBC in the cell lines investigated. This demonstrates that a dynamic approach for release of PEG from BC is beneficial to increase endosomal membrane disruptions with charged particles, as the presence of PEG can minimize membrane interactions in the absence of charge.[20]

It is of significant interest that our dual-cationic PICs suggest an endosomal escape mechanism for polyplexes which might be attributed to disruptions based on cationic-mediated cellular membrane interactions rather than through the PSE. In other words, selectively controlling interactions between polyplexes and the cell membrane is a new and facile approach for the design of effective and high-performance nonviral gene vectors. This results in nonviral vectors that are both safe to the cell while retaining high transfection efficiencies. Indeed, unlike PEI, which induces effective transfection activity but also causes high levels of nonspecific membrane-associated toxicity (Figure 2a), neutral shielded particles (BC, pH-PBC, and cov-PBC) result in cellular uptake with minimal toxicity to the membrane (Figure 2b–d). Upon sensing a decrease in pH, PEG chains are released from pH-PBC PICs, and the remaining BC particle acquires favorable cationic properties for disrupting endosomal membranes. After the particles escape into the cytosol (pH 7.4), hydrazide groups start to deprotonate upon sensing the new pH, imparting neutral properties to the PIC again. This is very similar to how natural viruses respond to their environment by exposing a fusogenic domain at low pH and concealing it at higher pH, and may explain the low metabolic toxicity of PICs in the cell.

Conclusions

In summary, we have designed an intelligent polycation with dual functional pK_a values capable of safely emulating the escape mechanism used by natural viruses. This novel dual-cationic block copolymer, poly(Asp-Hyd)-*b*-PLL, is pH-mediated to disrupt endosomal membranes based largely on charge interactions, and is therefore minimally toxic to the cell elsewhere. This is a mechanism separate from the traditional PSE followed by osmotic rupture of the vesicle. Furthermore, the significant presence of unconjugated hydrazides on the block copolymer can serve as a scaffold for easily incorporating many additional pH-sensitive functionalities, in addition to ALD-PEG, to the PIC to boost gene expression further. Examples of this include PEG-shielded fusogenic peptides for endosomal escape, nuclear localization signals (NLS), dynein-binding moieties, and additional masked targeting peptides for nuclear localization.[21,22] Therefore, these findings offer a new platform for generating more effective and complex multifunctional biomaterials for increasing gene expression.

Experimental Section

General materials. Branched polyethylenimine (M_W = 25000 g mol^{-1}) and poly(L-lysine) hydrobromide (M_W = 9200 g mol^{-1}) were purchased from Sigma–Aldrich (Milwaukee, WI, USA). All materials were used without further purification. The pDNA encoding firefly luciferase (pGL3, 5.3 kb) was obtained from Promega (Madison, WI, USA), transformed into electrocompetent DH5α cells, propagated in LB broth (1 L) supplemented with ampicillin (100 μg mL^{-1}), and purified with a plasmid Maxiprep kit (BioRad, Hercules, CA, USA). All pDNA had purity levels of 1.8 or greater by UV/Vis (A_{260}/A_{280}). For cell culture work, Dulbecco's modified Eagle's medium (DMEM), RPMI 1640, phosphate buffered saline (PBS), fetal bovine serum (FBS), trypsin–EDTA (0.25% trypsin, 2.21 mM EDTA in Hank's balanced salt solution (HBSS)) and penicillin/streptomycin were purchased from Cellgro (Mediatech, Herndon, VA, USA).

Physical characterization. pH titration measurements for polymers were obtained with an Orion micro-combination pH/sodium electrode (Thermo Electron Corporation, Waltham, MA, USA; see Supporting Information for general procedures). Dynamic light scattering and ζ potential data were obtained with a nanoZS 90 or a Malvern 3000HS series zetasizer (Malvern Instruments, UK). Polymers were mixed to form PICs at N/P = 20 by addition of polymer to an equal volume of pGL3 in Milli-Q water. The sample was allowed to incubate at room temperature for at least 15 min before dilution with the appropriate buffer ranging from pH 7.4 to pH 3.0. Particle diameters and ζ potentials were measured following dilution at each pH value.

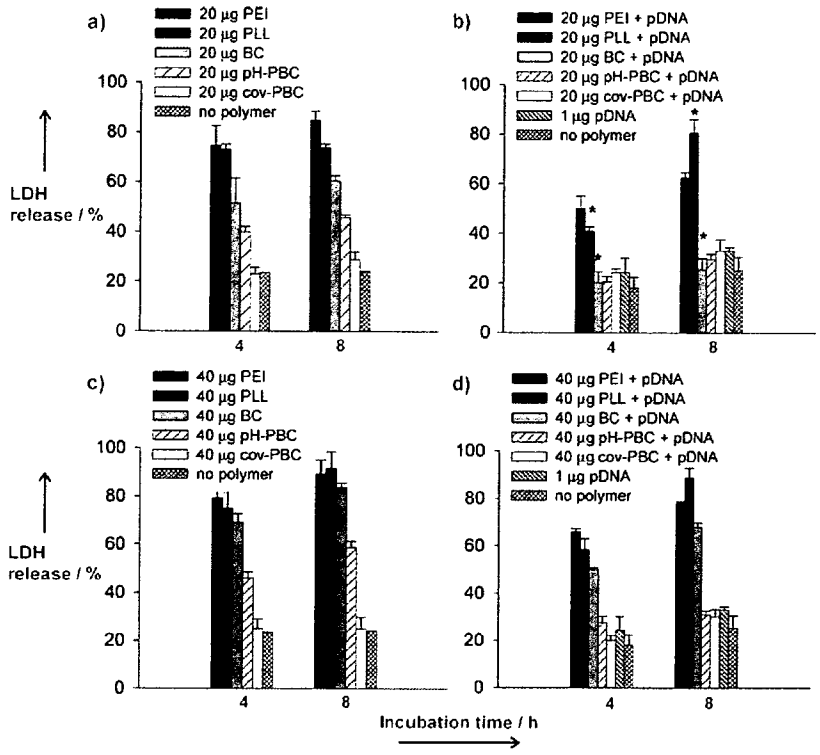

Figure 7. Membrane toxicity of polymers at concentrations of 20 and 40 μg mL^{-1} toward MDA-MB-231 (human breast cancer) cells in DMEM serum-free media. Polymers were incubated both in free form [parts a) and c)] and also pre-complexed to 1 μg pGL3 [parts b) and d)]. Free polymers with cationic components (PEI, PLL, BC) are toxic to cells after just 4 h incubation. However, complexed polymers with concealed PLL (BC, pH-PBC, cov-PBC) effect significantly less LDH release at 20 μg than the static polycations (*$p < 0.05$ using one-way ANOVA). At 40 μg, the presence of excess free polymers in solution with respect to pGL3 (see BC) re-establishes membrane toxicity.

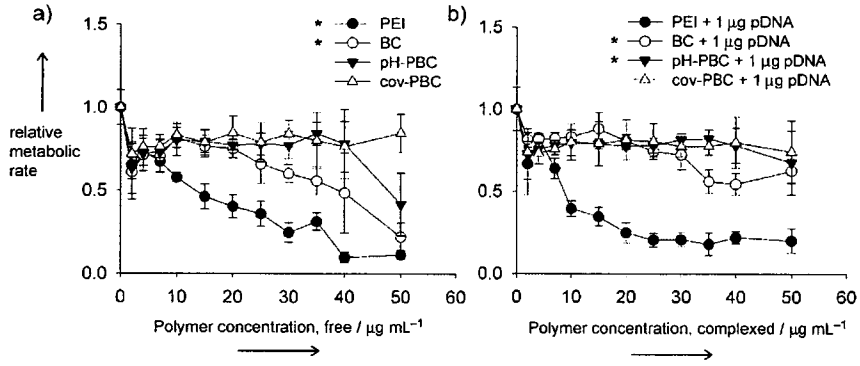

Figure 8. Metabolic toxicity of polymers incubated for 4 h at various concentrations toward MDA-MB-231 (human breast cancer) cells in DMEM serum-containing media. Polymers were incubated in both free form and pre-complexed to 1 μg pGL3. a) Free polymers with cationic components are toxic to cells at higher concentrations, with PEI being more toxic than BC (*$p < 0.05$ using two-way ANOVA). b) When complexed, BC results in negligible toxicity to the cell, similar to pH-PBC particles (*$p > 0.05$ using two-way ANOVA).

Cellular LDH release studies. Polymer interactions with cell membranes were evaluated by monitoring LDH release from MDA-MB-231 human breast cancer cells by using the CytoTox 96 non-radioactive assay from Promega (Madison, WI, USA). One-way ANOVA was used to statistically compare LDH data. MDA-MB-231 cells were seeded in 96-well plates at 25000 cells well^{-1}. After 18 h, the plates were washed with PBS (2×) and serum-free DMEM (90 μL) was added. Each 96-well plate was divided into two sections: maximum LDH and experimental LDH release. Polymer (free or complexed to 1 μg of pGL3) was added to both sections appropriately and incubated with the cells for 4 or 8 h. At the end of each incubation period, PBS was added to the experimental LDH wells (10 μL for volume correction) and 50 μL of the final supernatant was removed and put into a separate 96-well plate. Next, 10 μL of lysis solution (Triton-X, 9% *v/v*) was added to the remaining maximum release wells and incubated for 1 h at 37 °C. Then, 50 μL of the supernatants from these lysed cells were used as controls for determining maximum LDH release. LDH substrate (50 μL) was then added to the separate 96-well plates containing supernatants, covered with aluminum foil, and shaken at room temperature for 30 min before reading the absorbance ($\lambda = 492$ nm).

Cellular metabolic toxicity studies. Metabolic toxicity was assessed through the resazurin dye (Sigma–Aldrich, Milwaukee, WI, USA) by incubating the respective polymers (free or complexed with 1 μg pGL3) in serum-containing media and monitoring the toxic effects of the polymers on the metabolic rates of cells through reduction of the dye. Briefly, 96-well plates were seeded at 20000 cells well^{-1} and incubated for 24 h. Free polymer at increasing concentrations of 0–50 μg mL^{-1} was added to wells and incubated in serum-containing media for 4 h before refreshing the media. After 18 h incubation, 10 μL of resazurin dye (60 μM in PBS) was added to each well and incubated for 4 h before measuring fluorescence ($\lambda_{ex} = 560$ nm, $\lambda_{em} = 590$ nm). Cell viability is reported as relative metabolic rate with respect to controls without polymers. Two-way ANOVA was used to compare the data.

Cell transfection studies. MDA-MB-231 (human breast cancer), C2C12 (murine myoblast) and MCF-7 (human breast cancer) cell lines were obtained and cultured according to ATCC protocols. COS-7 cells (Green African monkey kidney) were obtained from David M. Lynn (University of Wisconsin). 4T-1 cells (murine colon cancer) were obtained from the Small Molecule Screening Facility

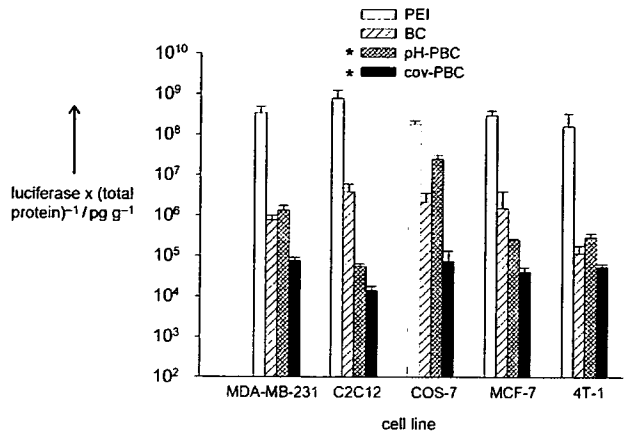

Figure 9. Transfection efficiency of the polymers in MDA-MB-231 (human breast cancer), C2C12 (murine myoblast), COS-7 (Green African monkey kidney), MCF-7 (human breast cancer) and 4T-1 (murine colon cancer) cells when incubated in the respective serum-containing media for 4 h. All polymers were formed at N/P = 20 (optimal ratio determined in tests with N/P = 7–50) with 2 μg pGL3. pH-PBC and BC PICs consistently effect significantly higher gene expression relative to cov-PBC across all cell lines (*$p < 0.05$ using one-way ANOVA in each case).

Center (University of Wisconsin) and cultured in RPMI 1640 supplemented with 10% FBS and 1% penicillin/streptomycin. The luciferase assay system was purchased from Promega. Luminescence was measured with a microplate Tropix luminometer (Applied Biosystems). Protein content was obtained using the DC protein assay kit from BioRad (Hercules, CA, USA), absorbance was measured with the Spectramax 190 microplate reader (Molecular Devices, Sunnyvale, CA, USA), and results were fit to a known protein calibration curve. Cells were seeded at either 300000 cells well^{-1} in 6-well plates or 150000 cells well^{-1} in 12-well plates and cultured for 24 h. The next day, wells were aspirated, washed with PBS (2 × 1 mL), and appropriate medium for each cell line was added (supplemented with 10% FBS and 1% penicillin/streptomycin). Complexes (2 μg pGL3 well^{-1}) formed at the indicated N/P ratio (N/P = 1 is defined as the minimum amount of polymer required to retard 1 μg of pGL3 on a 0.75% agarose electrophoretic gel) were added to wells 4 h before refreshing the media. After 12 h, plates were assayed with the Promega luciferase assay system. Luciferase relative light units (RLUs) were converted into units of concentration by using known luciferase concentration standards. One-way ANOVA was used to compare transfection data. A value of $p < 0.05$ was considered statistically significant.

Acknowledgements

This work was partially supported by NIH grant R01 AI-43346-08. M.P.X. acknowledges the NSF for an EAPSI fellowship to the University of Tokyo and the PhRMA foundation for a predoctoral fellowship in pharmaceutics.

Keywords: block copolymers · gene delivery · intracellular trafficking · nanoparticles · polymers

[1] M. L. Forrest, D. W. Pack, *Mol. Ther.* **2002**, *6*, 57–66.
[2] J. Rejman, V. Oberle, I. S. Zuhorn, D. Hoekstra, *Biochem. J.* **2004**, *377*, 159–169.
[3] F. M. Brodsky, C. Y. Chen, C. Knuehl, M. C. Towler, D. E. Wakeham, *Annu. Rev. Cell Dev. Biol.* **2001**, *17*, 517–568.
[4] O. Boussif, F. Lezoualc'h, M. A. Zanta, M. D. Mergny, D. Scherman, B. Demeneix, J. P. Behr, *Proc. Natl. Acad. Sci. USA* **1995**, *92*, 7297–7301.
[5] S. Fukushima, K. Miyata, N. Nishiyama, N. Kanayama, Y. Yamasaki, K. Kataoka, *J. Am. Chem. Soc.* **2005**, *127*, 2810–2811.
[6] M. Oishi, K. Kataoka, Y. Nagasaki, *Bioconjugate Chem.* **2006**, *17*, 677–688.
[7] Z. Y. Zhang, B. D. Smith, *Bioconjugate Chem.* **2000**, *11*, 805–814.
[8] G. F. Walker, C. Fella, J. Pelisek, J. Fahrmeir, S. Boeckle, M. Ogris, E. Wagner, *Mol. Ther.* **2005**, *11*, 418–425.
[9] J. P. Clamme, J. Azoulay, Y. Mely, *Biophys. J.* **2003**, *84*, 1960–1968.
[10] W. T. Godbey, K. K. Wu, G. J. Hirasaki, A. G. Mikos, *Gene Ther.* **1999**, *6*, 1380–1388.
[11] W. T. Godbey, K. K. Wu, A. G. Mikos, *Biomaterials* **2001**, *22*, 471–480.
[12] S. M. Moghimi, P. Symonds, J. C. Murray, A. C. Hunter, G. Debska, A. Szewczyk, *Mol. Ther.* **2005**, *11*, 990–995.
[13] K. Itaka, K. Yamauchi, A. Harada, K. Nakamura, H. Kawaguchi, K. Kataoka, *Biomaterials* **2003**, *24*, 4495–4506.
[14] Y. Bae, S. Fukushima, A. Harada, K. Kataoka, *Angew. Chem.* **2003**, *115*, 4788–4791; *Angew. Chem. Int. Ed.* **2003**, *42*, 4640–4643.
[15] Y. Bae, W. D. Jang, N. Nishiyama, S. Fukushima, K. Kataoka, *Mol. Biosyst.* **2005**, *1*, 242–250.
[16] Y. Nagasaki, T. Kutsuna, M. Iijima, M. Kato, K. Kataoka, S. Kitano, Y. Kadoma, *Bioconjugate Chem.* **1995**, *6*, 231–233.
[17] J. Rejman, A. Bragonzi, M. Conese, *Mol. Ther.* **2005**, *12*, 468–474.
[18] K. von Gersdorff, N. N. Sanders, R. Vandenbroucke, S. C. De Smedt, E. Wagner, M. Ogris, *Mol. Ther.* **2006**, *14*, 745–753.
[19] C. Goncalves, E. Mennesson, R. Fuchs, J. P. Gorvel, P. Midoux, C. Pichon, *Mol. Ther.* **2004**, *10*, 373–385.
[20] M. P. Xiong, M. L. Forrest, A. L. Karls, G. S. Kwon, *Bioconjugate Chem.* **2007**, *18*, 746–753.
[21] E. Mastrobattista, M. A. van der Aa, W. E. Hennink, D. J. Crommelin, *Nat. Rev. Drug Discovery* **2006**, *5*, 115–121.
[22] R. M. Sawant, J. P. Hurley, S. Salmaso, A. Kale, E. Tolcheva, T. S. Levchenko, V. P. Torchilin, *Bioconjugate Chem.* **2006**, *17*, 943–949.
[23] A. von Harpe, H. Petersen, Y. Li, T. Kissel, *J. Controlled Release* **2000**, *69*, 309–322.

Received: April 25, 2007
Revised: May 28, 2007
Published online on June 20, 2007

Supramolecular nanocarriers integrated with dendrimers encapsulating photosensitizers for effective photodynamic therapy and photochemical gene delivery†

Nobuhiro Nishiyama,[ac] Woo-Dong Jang[bd] and Kazunori Kataoka*[abd]

Received (in Montpellier, France) 3rd November 2006, Accepted 4th January 2007
First published as an Advance Article on the web 15th February 2007
DOI: 10.1039/b616050f

Recently, biomedical applications of dendrimers, three-dimensional tree-like macromolecules, have received much attention. In this paper, we introduce new biomedical applications of functional dendrimers: dendrimers encapsulating photosensitizers composed of a center dye molecule surrounded by poly(benzyl ether) dendrons with ionic peripheral groups as a new type of photosensitizer (PS) for photodynamic therapy (PDT). Dendrimers encapsulating porphyrin and with ionic peripheral groups (DPs) spontaneously formed polyion complex (PIC) micelles through electrostatic interactions with oppositely-charged block copolymers, and showed no self-quenching of the center dye molecule inside the micellar core due to a unique DP structure, leading to remarkable *in vitro* photocytotoxicity. The DP-incorporated micelles showed successful treatment of choroidal neovascularization (CNV) in rats without any sign of side effects. Thus, the DP-incorporated micelles are expected to be an innovative PS formulation for successful PDT against ophthalmic diseases. In this paper, we also review polymeric micelles incorporating phthalocyanine core dendrimers (DPc) for cancer PDT and novel light-responsive supramolecular gene carriers integrated with DPc for site-directed transfection *in vivo*.

[a] *Center for Disease Biology and Integrative Medicine, Graduate School of Medicine, The University of Tokyo, 7-3-1 Hongo, Bunkyo-ku, Tokyo 113-0022, Japan. E-mail: kataoka@bmw.t.u-tokyo.ac.jp; Fax: +81-3-5841-7139; Tel: +81-3-5841-7138*
[b] *Department of Materials Science and Engineering, Graduate School of Engineering, The University of Tokyo, 7-3-1 Hongo, Bunkyo-ku, Tokyo 113-8656, Japan*
[c] *Center for NanoBio Integration, The University of Tokyo, 7-3-1 Hongo, Bunkyo-ku, Tokyo 113-8656, Japan*
[d] *Department of Chemistry, College of Science, Yonsei University, 134 Sinchondong, Seodaemun-gu, Seoul 120-749, Korea*
† This paper was published as part of the special issue on Dendrimers and Dendritic Polymers: Design, Properties and Applications.

Introduction

Photodynamic therapy (PDT) has been attracting increasing attention as a promising method for the treatment of solid tumors and ophthalmic diseases.[1-3] PDT involves administration of photosensitizers (PSs) to the body, followed by activation of PSs at the diseased site using light of specific wavelength. Upon photoirradiation, PSs undergo photosensitized reaction processes of type I and type II. The former produces free radicals or superoxide anions resulting from hydrogen- or electron transfer from the photoexcited PSs,

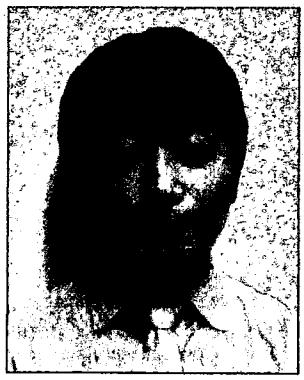

Nobuhiro Nishiyama, PhD, is an Assistant Professor of Clinical Biotechnology at the Graduate School of Medicine of the University of Tokyo, Japan. He received a PhD degree in Materials Engineering from the University of Tokyo in 2001. He was a Postdoctoral Fellow at the University of Utah and an Assistant Professor at the University of Tokyo Hospital. His main research interest concerns the biomedical applications of intelligent nanodevices for drug and gene delivery.

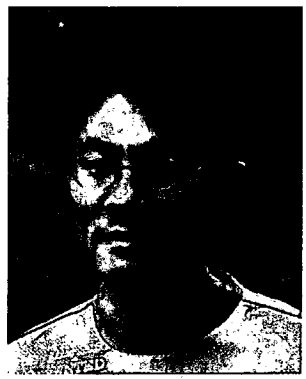

Woo-Dong Jang, PhD, is an Assistant Professor at the Chemistry Department of Yonsei University, Korea. He received a BSc degree in Polymer Chemistry from Kyoungpook National University, Korea, and a PhD degree in Chemistry and Biotechnology from the University of Tokyo, Japan. He was a Postdoctoral Fellow at the Japan Science and Technology Agency and an Assistant Professor at the University of Tokyo. His main research interest concerns the biomedical application of polymeric materials.

whereas the latter generates cytotoxic singlet oxygen ($^1O_2$) by the energy transfer. In general, the type II reaction is known to be more efficient in PDT.

A challenge in PDT is to create efficient PSs, which show highly selective photocytotoxicity to the diseased tissues, and an increasing number of PSs are presently being explored in preclinical and clinical studies.[1,2] PSs generally have large π-conjugation domains, such as a porphyrin structure, to obtain a high quantum yield and effective energy absorption. Therefore, most conventional PSs easily form aggregates in aqueous media through their π–π stacking and hydrophobic interactions, resulting in the self-quenching of the excited state. This may decrease the photodynamic effect of the PS after its accumulation in the diseased tissue. On the other hand, there is also a strong incentive to develop effective drug delivery systems (DDS) for PSs, to enhance the selectivity and effectiveness of PDT as well as prevent side effects caused by non-specific distribution of PSs in the body, such as prolonged skin hypersensitivity to sunlight.[2] To date, a variety of DDS, including polymer–PS conjugates,[4] long-circulating liposomes[5] and polymeric micelles,[6] have been examined; however, the aforementioned properties of PSs, *i.e.*, a strong tendency to form aggregates and the related self-quenching effect, might interrupt the development of effective PS formulations. In general, it might be difficult to effectively incorporate such hydrophobic substances into drug carriers. Also, increased loading of PSs into drug carriers could change the modality of photochemical reaction from type II to type I due to aggregate formation, leading to diminished photodynamic efficacy.[7] Thus, both efficiencies of the PS delivery and photochemical reactions of PS itself should be considered in the development of DDS in PDT.

Recently, we have developed a new type of PS based on a dendritic architecture, *i.e.*, dendrimers encapsulating porphyrin with ionic peripheral groups (DPs), in which the centre porphyrin is surrounded by the 3rd generation of poly(benzyl ether) dendrons (Fig. 1).[8] Unlike conventional PSs, DPs ensure a high efficacy of singlet oxygen production even at a high concentration, since the dendritic envelopes of DPs can prevent aggregation of the center porphyrin (Fig. 2). Thus, it is assumed that the encapsulation of DPs into drug carriers might not compromise the singlet oxygen production efficiency. In addition, the peripheries of DPs can be modified with a variety of functional groups, providing water-solubility and practical functions such as tissue-targetability. Also, the introduction of charged ionic groups into the periphery of a DP allows its stable incorporation into a supramolecular nanocarrier, a polyion complex (PIC) micelle, through electrostatic interactions with oppositely-charged block copolymers as schematically shown in Fig. 2.

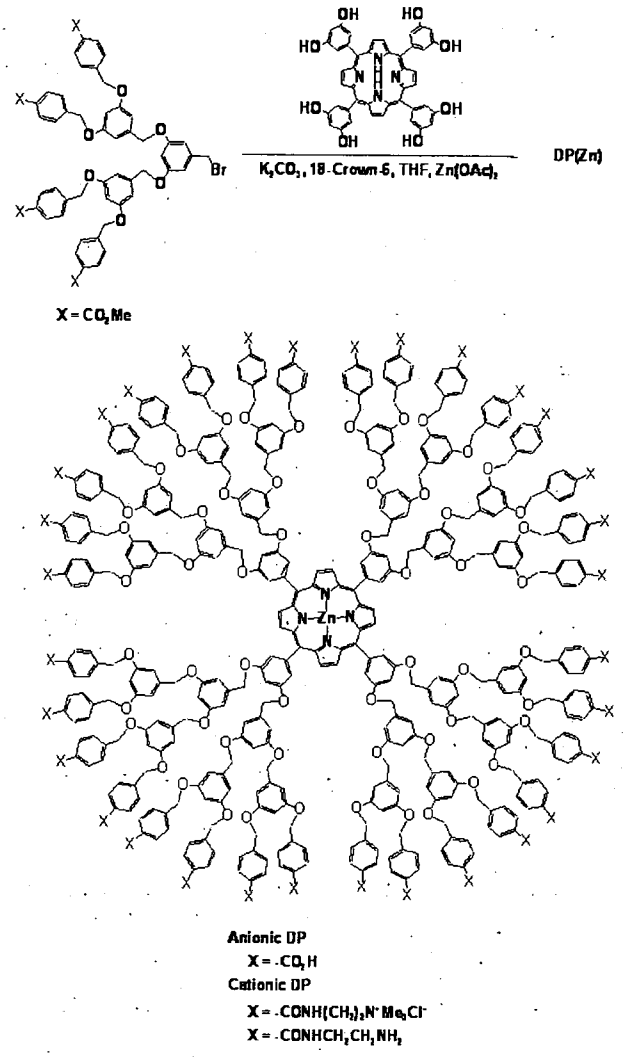

Fig. 1 Chemical structures of dendrimers encapsulating porphyrin with ionic peripheral groups (DPs) and the synthetic scheme.

Polymeric micelles, self-assemblies of block copolymers, are characterized by a size of several tens of nanometres, a fairly narrow size distribution, remarkably low critical micelle concentration (c.m.c.) and segregated core–shell structure, and they have recently received considerable attention as a promising modality of drug carriers.[9–11] It has been demonstrated that polymeric micelles could circulate stably in a bloodstream and, therefore, accumulate effectively in solid tumors[12] due to the enhanced permeability and retention (EPR) effect, characterized by microvascular hyperpermeability and impaired lymphatic drainage in tumor tissues.[13] Also, we have

Kazunori Kataoka, PhD, is a Professor of Biomaterials at the Graduate School of Engineering of the University of Tokyo, Japan. Since 2004, he has also held a joint position at the Graduate School of Medicine of the University of Tokyo as a Professor of Clinical Biotechnology. He received a PhD from the University of Tokyo in 1979. Dr Kataoka is the author of more than 350 scientific papers in international journals and a recipient of many awards. His current major research interests include the development of new polymeric carrier systems, especially block copolymer micelles, for drug and gene targeting.

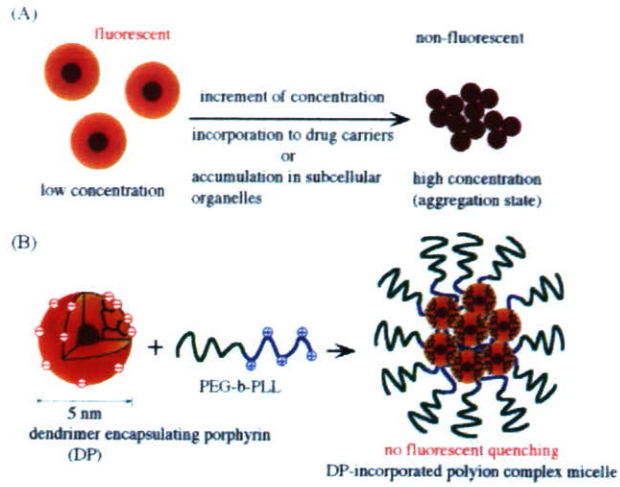

Fig. 2 (A) Conventional PSs form aggregates at a high concentration, resulting in their self-quenching. (B) Formation of DP-incorporated polyion complex (PIC) micelles through electrostatic interactions between anionic DPs and poly(ethylene glycol)-*block*-poly(L-lysine) (PEG-*b*-PLL) copolymers. The dendritic structure of DP can sterically prevent aggregation of the center porphyrin, thus there is no fluorescent quenching of the center porphyrin. [Ref. 12, copyright permission from Wiley-VCH].

recently reported that polymeric micelles also accumulated in the choroidal neovascularization (CNV) site in rat models,[14] suggesting the targeted therapy of ophthalmic diseases by polymeric micelles. The PIC micelle, a new type of polymeric micelle formed through the electrostatic interaction between a pair of charged block copolymers and oppositely-charged macromolecules,[15] is expected to be a targetable carrier system for biologically active molecules, including proteins[16] and nucleic acids[17,18] as well as ionic DPs.[19 22]

In this paper, we review recent advances in the field of PIC micelles incorporating photosensitizer core dendrimers for effective PDT. Also, we introduce our new technology for the control of transgene expression by using gene nanocarriers integrated with dendrimers encapsulating photosensitizers.

Dendrimers encapsulating porphyrins (DPs) as a new photosensitizer

Synthesis of ionic DPs

There are two different synthetic strategies towards ionic DPs; a divergent and a convergent growth approach are generally employed to construct dendrimer frameworks.[23] DPs have poly(benzyl ether) dendritic wedges, which were first synthesized by Fréchet and Hawker using the convergent approach.[24] Aida *et al.* reported the first example of a dendrimer encapsulating a metalloporphyrin, in which the zinc porphyrin functionality is covalently encapsulated by poly(benzyl ether) dendritic wedges with methoxycarbonyl groups on the exterior surface, on the basis of Fréchet and Hawker's convergent approach.[25] Fig. 1 shows the synthetic scheme towards DPs. Alkaline-mediated coupling of 5,10,15,20-tetrakis(3′,5′-dihydroxyphenyl)porphine with methoxycarbonyl-terminated aryl ether dendritic bromides gave a DP, which was metalated with $Zn(OAc)_2$, followed by hydrolysis of the exterior MeO_2C-groups with KOH. Dialysis of the reaction mixture for 2 days in fresh water to remove excess KOH, followed by evaporation to dryness, gave an anionic DP bearing 32 carboxylic groups on the periphery. Also, the synthesis of a cationic DP, bearing 32 quaternary ammonium groups on the periphery, was performed by amidation of the anionic DP with 1-amino-2-(trimethylammonium)ethane, followed by purification by column chromatography and preparative HPLC using THF as an eluent. Likewise, a DP bearing 32 primary amino groups was prepared by amidation of the anionic DP with *N*-(trifluoroacetyl)ethylene-1,2-diamine, followed by quantitative deprotection of the trifluoroacetyl group. The perfection of cationic DPs after amidation of anionic DP was confirmed by MALDI-TOF-MS.[21]

Properties of ionic DPs as a photosensitizer for PDT

As described in the Introduction, DPs show a unique photochemical property that the center porphyrin might not be quenched even at a high concentration due to its spatial isolation in the focal core of the dendrimer. Thus, the photochemical reaction of DPs may not be affected by their subcellular localization and local concentrations. Regarding the photochemical properties, ionic DPs absorb light at 415, 434 (Soret bands) and 559 nm (Q-band) and emit fluorescent light at 610 and 660 nm. In our previous study, the singlet oxygen quantum yield of DPs was measured by direct observation of the O_2 ($^1\Delta_g$) → O_2 ($^3\Sigma_g^-$) transition at 1270 nm ((0,0) vibronic band) in MeOD.[8] It was demonstrated that ionic DPs showed similar singlet oxygen quantum yield to a conventional PS, protoporphyrin IX. Thus, the center porphyrin possesses a high singlet oxygen quantum yield in spite of its dendritic structure. In the photodynamic action of DPs, only the singlet oxygen or other reactive oxygenic species (ROS) is assumed to play an essential role, because the direct interaction of dye radicals with other compounds should be minimal in the dendritic architecture. Also, DPs may be hardly photobleached during photochemical reactions, although this effect remains to be elucidated. It is generally known that singlet oxygen has a quite short lifetime in an aqueous milieu, and the diffusion distance of $^1O_2$ is estimated to be less than 10 nm.[2] Nevertheless, the 3-D structure of dendrimers with the size of 5 nm appeared not to be a barrier for the $^1O_2$-induced photodynamic effect, because ionic DPs showed comparable or even more efficient photocytotoxicity compared with conventional PSs.[8] Possibly, the lifetime of $^1O_2$ may be prolonged inside the hydrophobic dendritic structure of DPs.

DPs are hydrophilic macromolecules (~5 nm), so that they are assumed to be taken up by the cells through endocytic pathways. Nevertheless, the ionic DPs showed different cellular associations depending on the peripheral charged groups. In our previous study, cationic DP showed rapid association to the negatively-charged plasma membrane through electrostatic interaction, followed by internalization by adsorptive endocytosis, whereas anionic DPs were slowly internalized by fluid phase endocytosis due to the electrostatic repulsion.[8] Thus, both cationic and anionic DPs finally localized in

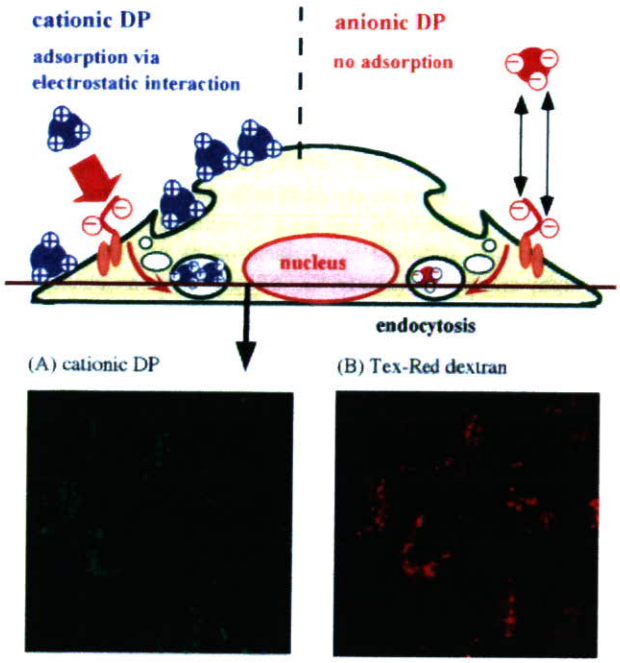

Fig. 3 Schematic illustration of the cellular association manners of cationic and anionic DPs, and confocal images of cationic DP (A) and Tex-Red dextran, an endocytosis marker (B) in LLC cells after incubation for 3 h at 37 °C. [Ref. 8, copyright permission from American Chemical Society].

endosomal compartments, as demonstrated by colocalization with Tex-Red dextran, a fluid phase endocytic marker (Fig. 3). Although cationic DP showed only 22–25 times higher cellular association than anionic DP, the photocytotoxicity ($^1O_2$-induced cytotoxicity) of cationic DP was 230 times higher than that of anionic DP.[8] Such a difference in the photocytotoxicity between cationic and anionic DPs may be due to different interactions of both compounds with cellular components. That is, cationic DP is likely to electrostatically interact with negatively-charged cell membranes, photodamaging membrane components, which may be susceptible to $^1O_2$-induced cell death.

Fluorescent microscopy observation using organelle-specific dyes revealed that the photodamage by DPs maintained the characteristic structure of cell membranes and intracellular organelles (the plasma membrane, mitochondrion and lysosome), whereas such organelles were severely photodisrupted by conventional PSs.[8] Nevertheless, cationic DP induced efficient cell death. In this regard, the fluorescence of Rhodamine 123 (Rh123), a mitochondrion marker, was significantly attenuated by the photodamage by cationic DP. The fluorescence intensity of Rh123 is known to be correlated with the amount of adenosine triphosphate (ATP) in the cell.[26] Therefore, cationic DP may have clipped ATP production in the cell, leading to efficient cell death. The eliminated ATP production may be caused by exhaustion of intracellular oxygen or photodamage to the plasma membrane.[27,28] Also, there is another possibility that the photodamage to the cell membranes could disrupt the endosome/lysosome, localizing DPs in cytoplasmic organelles, which are susceptible to $^1O_2$-induced cell death.[29] For example, it was reported that the photodamage to the mitochondrion induced apoptosis through the cytoplasmic release of cytochrome c.[30] The exact molecular target of ionic DPs is an issue to be clarified in the future.

Low dark toxicity of PS is one of the important criteria for assessing the usefulness of PS because unwanted toxicity to normal tissues is one of major side effects in clinical PDT.[31] Ionic DPs showed extremely low dark toxicity even after prolonged incubation of 72 h.[8] The extremely low dark toxicity of DPs may result from the distinctive intracellular disposition characteristics due to their relative large size (~5 nm).

DP-incorporated polyion complex (PIC) micelles for effective PDT

Physicochemical properties of DP-incorporated PIC micelles

The DP-incorporated PIC micelles are formed from a pair of charged block copolymers of poly(ethylene glycol)-*block*-poly(L-lysine) (PEG-*b*-PLL) or poly(ethylene glycol)-*block*-poly(aspartic acid) (PEG-*b*-PAA) and oppositely-charged DPs with 32 charged groups on the periphery (Fig. 2B). Simple mixing of block ionomers and ionic DPs at a stoichiometric charge ratio led to the spontaneous formation of the PIC micelles. The PIC micelles prepared from negatively-charged DP and positively-charged PEG-*b*-PLL had a diameter of approximately 64 nm with an extremely narrow size distribution in physiological saline solution. The spherical shape of the DP-incorporated micelles was confirmed by observation with atomic force microscopy (AFM) and field emission-transmission electron microscopy (FE-TEM). The static light scattering (SLS) measurement revealed that an individual PIC micelle contains an average of 38 DP molecules.[19] From the standpoint of the application as drug carriers, the stability of the PIC micelles against salt concentrations might be primarily important, since the electrostatic shielding of polyelectrolytes with salt ions might destablize the PIC structure.[32] In this regard, the PIC micelles consisting of cationic DP bearing 32 quaternary ammonium groups–PEG-*b*-PAA showed a higher stability against NaCl concentrations than those of PLL_{27}–PEG-*b*-PAA.[19] This may be explained by the assumption that the PIC from a rigid dendrimer may produce a smaller entropy gain upon dissociation than that from a flexible PLL homopolymer. In the case of the PIC micelles consisting of cationic DP bearing 32 primary amino groups–PEG-*b*-PAA or anionic DP–PEG-*b*-PLL, the complexation between DPs and block copolymers might be accomplished by the formation of hydrogen bonds between carboxylic acid and primary amine groups after proton transfer from the acid amine. Therefore, the resulting polyion complex micelles showed a remarkable stability against an increase in NaCl concentrations up to 1500 mM, 10 times higher than the physiological concentration.[19,21]

The PIC micelles of anionic DP–PEG-*b*-PLL showed pH-dependent structural changes.[22] In this study, the translational diffusion coefficient (D_T) and normalized $(Kc/\Delta R(0))^{-1}$ (normalized to the micelle at pH 7.4) of the PIC micelles, where D_T is related to the hydrodynamic diameter based on

the Stokes–Einstein equation, and the normalized $(Kc/\Delta R(0))^{-1}$ value is related to the changes in the apparent molecular weight of the micelles, were measured under different pH conditions by dynamic light scattering (DLS) and SLS measurements, respectively. Both the hydrodynamic diameter and normalized $(Kc/\Delta R(0))^{-1}$ value remained constant in the pH range from 6.4 to 8.5. However, when the pH was below 6.4, the PIC micelles showed a gradual increase in the diameter and apparent molecular weight, and finally underwent precipitation at pH 5.6, indicating the acid-responsive feature of the micelles. Under acidic pH conditions, the carboxylic acid groups of DP might be considerably protonated, leading to diminution of the electrostatic interaction between anionic DP and PEG-*b*-PLL, thus the well-defined core–shell structure may become more obscure and a merging of the micelles may take place. The similar pH-dependent structural changes of the PIC micelles were also observed for the system of cationic DP bearing 32 primary amino groups–PEG-*b*-PAA.[21] Such a pH-responsive behavior of the micelles allows their effective accumulation in solid tumors in response to a low pH condition in the tumor tissue (~pH 6.5)[33] or an intracellular acidic endosomal compartment (~pH 5.0) while their stable circulation in the bloodstream is expected.

In vitro photodynamic effect of DP-incorporated PIC micelles

In the UV-Vis absorption spectra, the PIC micelles of anionic DP–PEG-*b*-PLL showed a red shift of 5 nm for the Soret band of the porphyrin core and a hypochromicity of about 5%,[22] which seems to be consistent with the previous reports on the electrostatic assembly of charged porphyrins and oppositely-charged compounds.[34,35] The cancellation of the charge repulsion of the negatively-charged DP surface by the formation of the electrostatic assembly may lead to shrinkage of the hydrophobic dendrimer frameworks, which may be related to the hypochromicity.[25] Importantly, the PIC micelles showed no fluorescent quenching of DP (630 nm), although the local concentration of DP is assumed to be extremely high in the core of the PIC micelles.[22] Similarly, no fluorescent quenching of DP in the PIC micelles was observed for the system of cationic DP bearing 32 primary amine groups–PEG-*b*-PAA.[21] It is worth noting that no fluorescent quenching of DP was microscopically observed inside the cell incubated with the DP-incorporated PIC micelles,[22] suggesting the effective photochemical reaction in the living cell directed the enhanced photocytotoxicity. It is hypothesized that the dendritic envelope of DP might prevent the collisional quenching of the center porphyrin even at an extremely high concentration. This unique photochemical property of the DP-incorporated PIC micelles might not be achieved by other conventional PSs and PS formulations.

In regard to the efficiency of the photochemical reactions, the DP-incorporated PIC micelles showed an oxygen consumption rate comparable to free DP in phosphate-buffered saline containing fetal bovine serum (FBS) as a singlet oxygen acceptor (Fig. 4).[22] This result suggests that the singlet oxygen molecules produced from DP can escape from the micellar structure and react with proteins of FBS. Thus, the DP-incorporated PIC micelles might have the capacity to efficiently photo-oxidize biomolecules in the solution without their structural changes. Possibly, the DP-incorporated PIC micelles may achieve the elevated concentration of local singlet oxygen, which may not be obtained by other formulations containing conventional PSs.

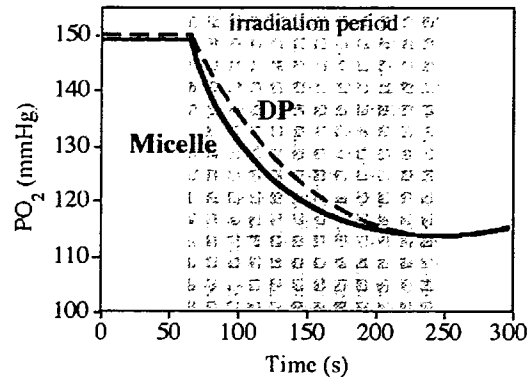

Fig. 4 Profiles of the oxygen consumption by anionic DP (--) and the DP-incorporated micelles (—) in phosphate-buffered saline solution containing 10% fetal bovine serum (FBS). The light irradiation and the oxygen partial pressure measurement were performed using an Hg lamp and a Clark-type oxygen microelectrode, respectively. [Ref. 12, copyright permission from Wiley-VCH].

Very interestingly, the PIC micelles of anionic DP–PEG-*b*-PLL showed approximately 280 times more efficient photocytotoxicity (against Lewis lung carcinoma (LLC) cells) compared with free anionic DP (Fig. 5), although incorporation of DP into the PIC micelles resulted in an only 6–8 times increase in the cellular uptake.[22] From a practical standpoint, such a manner of the photocytotoxicity enhanced by the micelle formulation may avoid long-term phototoxicity after PDT, since the DP-incorporated micelles are assumed to gradually dissociate to constituent DP and block copolymers in the body. It may be hypothesized that the DP-incorporated

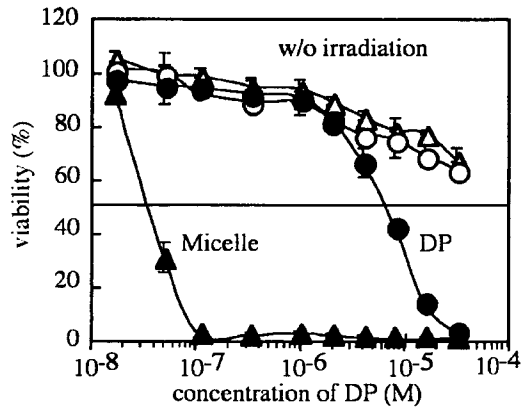

Fig. 5 The photocytotoxicity (closed symbols) and the dark toxicity (open symbols) of anionic DP (circles) and the DP-incorporated micelles (triangles) against LLC cells. In this assay, the cells were photoirradiated for 10 min with broadband visible light using a xenon lamp (150 W) equipped with a filter passing light of 400 700 nm (fluence: 180 kJ cm^{-2}). The cell viability was evaluated by the 3-(4,5-dimethylthiazol-2-yl)-2,5-diphenyltetrazolium bromide (MTT) assay.

micelles may have a specific mechanism to enhance their photocytotoxicity. Recently, PEGylated chlorin-e_6 as well as PEG-based polymeric micelles were reported to show enhanced localization in several cytoplasmic organelles, including the mitochondrion.[30,36] Thus, the PEG shell of the PIC micelles may have a role in altering the intracellular mechanism of DP to increase the photocytotoxicity. Otherwise, the photodamage-induced disruption of the endosomal/lysosomal membranes may assist the localization of DP in the cytoplasmic organelles, which may be susceptible to $^1O_2$-induced cell death. In any case, the remarkably increased concentration of local singlet oxygen by encapsulation into the PIC micelles is likely to contribute significantly to the enhanced photocytotoxicity of DP. Further investigations to address the detailed mechanisms of the enhanced photocytotoxicity of the DP-incorporated micelles are now in progress in our research group.

PDT using DP-incorporated PIC micelles

The exclusive age-related macular degeneration (AMD), a condition caused by choroidal neovascularization (CNV), is a leading cause of visual loss in developed countries.[3] Recently, Visudyne®, a liposomal formulation of verteporfin, has been demonstrated to be effective for the treatment of AMD, and has been approved for clinical use.[37] However, PDT with Visudyne requires repeated treatments every three months, and many patients nevertheless suffer from visual loss due to recurrence of CNV. Therefore, there is a strong incentive to develop more effective formulations of PSs for the PDT treatment against AMD.

Recently, we applied the PIC micelles of anionic DP–PEG-*b*-PLL for PDT of experimental CNV in rats, which was created by laser photocoagulation.[38] When DP-incorporated micelles were intravenously administered, they showed effective and selective accumulation in the CNV lesions.[38] Laser irradiation (5–50 J cm^{-2}) at 4 h after iv administration of DP-incorporated micelles resulted in successful occlusion of CNV in 60–72% of the tested animals. Importantly, approximately 80% of the tested animals showed maintained CNV occlusion even 7 days after laser irradiation.[38] In contrast, it was reported that PDT with Visudyne under the same experimental conditions showed less effectiveness in CNV occlusion and resulted in recurrence of CNV 7 days after the treatment.[39] Thus, DP-incorporated micelles might be an effective PS formulation, and may not require the repeated treatments, which are problems of other PS formulations. In this study, the skin photodamage was also evaluated by photoirradiating the mouse abdominal skin with broadband visible light (Xenon lamp equipped with a filter passing light of 377–700 nm) 4 h after iv injection of DP-incorporated micelles or Photofrin, a clinically used PS formulation for cancer therapy. As a result, mice treated with DP-incorporated micelles did not experience macroscopically observable skin damage, whereas those treated with Photofrin displayed severe skin damage.[38] Thus, DP-incorporated micelles might circumvent skin hyperphotosensitivity, a major side effect of current PDT, due to their reduced accumulation in the skin. From these *in vivo* results, we can conclude that DP-incorporated micelles may have an innovative PS formulation for the treatment of ophthalmologic diseases.

Dendrimer encapsulating phthalocyanine as a photosensitizer for cancer therapy

We have demonstrated that DP-incorporated micelles are a potent PS formulation for PDT against ophthalmologic diseases. However, DPs have relatively short excitation wavelengths (*i.e.*, 430 and 560 nm), which might be a limitation for PDT except for the transparent tissues such as ophthalmologic organs. Skin tissue has melanin dyes, which absorb short wavelength light to prevent photochemical genetic disorder, and also heme proteins of red blood cells account for most of the light absorption in the visible region. Such light absorption by human bodies prevents the excitation of PSs for photochemical reactions. Therefore, PSs should have long absorption wavelength for the PDT of deeper lesions such as solid tumors.

In this regard, several phthalocyanine molecules have been widely studied as potential PSs with an appropriate absorption wavelength for practical PDT application.[2,40] The phthalocyanines have an optical absorption at approximately 680 nm, where the light can penetrate tissues 2 times deeper than Photofrin (630 nm). Recently, we have synthesized dendrimers encapsulating phthalocyanine with ionic peripheral groups (DPc, Fig. 6) with the maximum absorption at 685 nm according to the synthetic procedure established by Ng *et al.*,[41] and prepared DPc-incorporated micelles, having the size of approximately 50 nm, through the electrostatic interaction between anionic DPc and PEG-*b*-PLL.[42] DPc-incorporated micelles were stable in a phosphate-buffered solution containing 10% FBS, maintaining the size and polydispersity of the micelles. The micelle formation was accompanied by a shift of maximum absorption wavelength of DPc from 685 nm

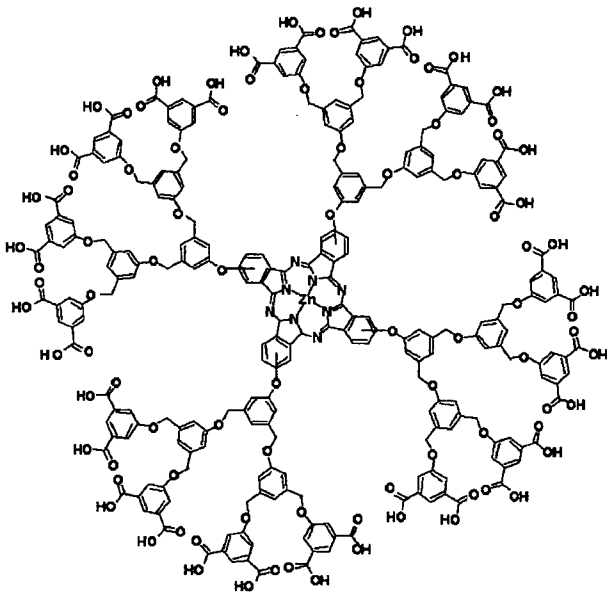

Fig. 6 Chemical structure of dendrimer encapsulating phthalocyanine (DPc).

to 630 nm, indicating some interactions between the phthalocyanine units of DPc (*i.e.*, aggregate formation) in the micellar core. The relatively small dendritic wedges may be insufficient to prevent such interactions. As a result, DPc-incorporated micelles showed reduced oxygen consumption rates compared with DPc alone.[42] Nevertheless, DPc-incorporated micelles showed significant enhancement of the light-induced cytotoxicity, which greatly relied on the photoirradiation time. In contrast, free DPc did not exhibit such enhancement of the photocytotoxicity regardless of irradiation time. Thus, DPc-incorporated micelles achieved approximately 100-fold photocytotoxicity compared with free DPc after 60 min photoirradiation. The treatment of solid tumors by PDT with DPc-incorporated micelles is ongoing in our laboratory, and the results will be reported elsewhere in the near future.

Photochemical gene delivery using dendrimer encapsulating phthalocyanine (DPc)

The DPc-incorporated micelles are taken up by the cells through the endocytic pathway, preferentially localizing in the endosome or lysosome. Upon photoirradiation, DPc-incorporated micelles may photochemically disrupt the endosomal/lysosomal membrane to relocalize in the subcellular organelles susceptible to $^1O_2$-induced cell death. This process is available for the light-induced cytoplasmic delivery of macromolecular compounds such as plasmid DNA (pDNA), which are impermeable to cell membranes and easily digested in the endosome or lysosome. This concept was "photochemical internalization (PCI)" by Berg and Høgset *et al.*[29,43–46] It should be noted that the light dose necessary for PCI is much lower than that for PDT, ensuring the low photocytotoxicity of PCI. Recently, we also carried out *in vitro* PIC-mediated gene transfection using a combination of the DPc–PEG-*b*-PLL and pDNA–PEG-*b*-PLL micelles, and achieved 100-fold photochemical enhancement of the transgene expression while maintaining 80% cell viability over a wide range of DPc concentrations and light doses.[47] Moreover, we optimized the chemical structures of PEG-*b*-polycations forming the pDNA-incorporated micelles for the PCI-mediated transfection, and found that the use of PEG-*b*-polycations having the repeated ethylenediamine units in the side chain allowed approximately 1000-fold light-selective gene transfection,[48] suggesting that the PCI and the so-called proton sponge effect[49] may work synergistically to enhance the transfection efficiency.

From the standpoint of *in vivo* applications of the PCI-mediated transfection, gene carriers should be equipped with a photosensitizing unit as one component, motivating us to develop the ternary complexes composed of pDNA, quadruplicated cationic peptide (CP_4) containing nuclear localization signal (NLS) sequence and anionic DPc (Fig. 7).[50] The simple addition of anionic DPc to the cationic pDNA–CP_4 complexes led to the spontaneous formation of the ternary complexes having the pDNA–CP_4 core surrounded by the DPc envelope, and the obtained nanoparticles had the size of 130 nm with a narrow distribution. Interestingly, such nanoparticles were not obtained by the addition of poly(aspartic acid) homopolymer with a polymerization degree of 26 to the pDNA–CP_4 complexes, suggesting that the 3-D structure of DPc might play an essential role in the formation of the ternary complexes. Also, such ternary complexes are definitely discriminated from the layer-by-layer assemblies,[51,52] because a core of hard materials is not required for the formation of the ternary complexes. The pDNA–CP_4–DPc ternary complexes are assumed to activate the transgene expression in a light-inducible manner according to the following processes: (1) internalization of the ternary complexes through endocytosis, (2) release of DPc from the ternary complexes due to protonation of the peripheral carboxyl groups of DPc under acidic conditions in the endosome, (3) interaction with the endosomal membrane due to the hydrophobic nature of the dendrimer framework, (4) light-induced endosomal escape of the pDNA–CP_4 complexes through the photochemical disruption of the endosomal membrane, and (5) nuclear transport of the pDNA–CP_4 complexes guided by the NLS sequence.[53] As a result, the ternary complexes showed a more than 100-fold light-induced enhancement of *in vitro* transgene expression while maintaining the cell viability.[50] The PCI-mediated transfection with the ternary complexes was not accompanied by long-term toxicity, which was observed by transfection using polyethylenimine (PEI), a well-known highly transfectable polycation. Thus, the ternary complexes might avoid the cytotoxicity induced by buffering polycations, because the cytotoxic events might occur only during the photoirradiation. To demonstrate the potential of the ternary complexes for *in vivo* gene transfer, the ternary complexes were subjected to subconjunctival injection in rats, followed by laser irradiation with a semiconductor laser (689 nm) at 2 h post-injection (Fig. 8). The PCI-mediated gene transfer with the ternary complexes resulted in appreciable gene expression of the fluorescent protein (*Venus*) only at the laser-irradiated site in the conjunctiva.[50] In contrast, the subconjunctival injection of the pDNA–PEI complexes failed

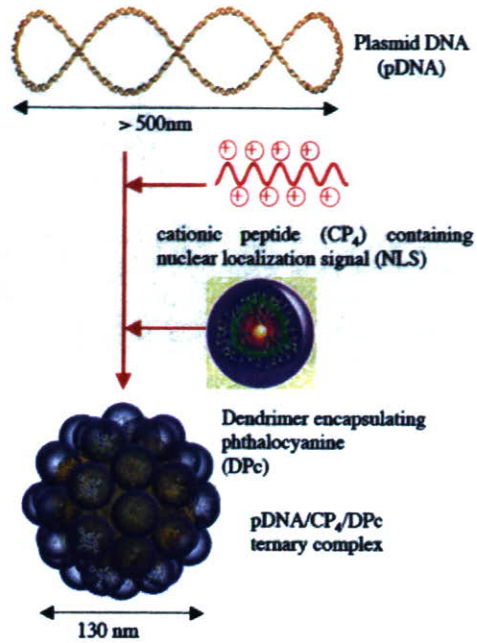

Fig. 7 Formation of the pDNA CP_4 DPc ternary complexes as light-responsive gene carriers for site-directed gene transfer.

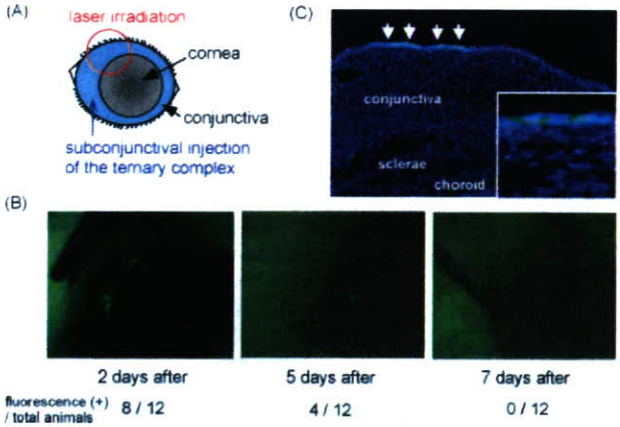

Fig. 8 Light-induced gene transfer to the rat conjunctival tissue. (A) Scheme for *in vivo* transfection. Rats were given a subconjunctival injection (colored in light blue) of the ternary complexes containing pDNA encoding a fluorescent protein, *Venus*. At 2 h post-injection, a part of the conjunctiva (red circle) was irradiated by the laser. (B) Fluorescent images of *Venus* expression in the rat eye at 2, 5 and 7 days after the transfection. The rates of the fluorescent-positive eyes (fluorescent (+)/total eyes) are indicated below the images. (C) Fluorescent image of the *Venus* expression at 2 days after the transfection in the frozen section of the conjunctival tissue. The cell nuclei were stained in blue. [Ref. 50.]

in the gene transfection. Thus, we succeeded in the control of the *in vivo* transgene expression by using light-responsive gene carriers integrated with DPs.

Future prospects

In this paper, we have reviewed the characteristics of the DP-incorporated PIC micelles from the standpoint of the photochemical reactions and *in vitro* and *in vivo* photodynamic effect. Our results revealed that the DP-incorporated micelles possess unique photochemical properties and show remarkable *in vitro* photodynamic effect, which have not been achieved by other PS formulations. The PDT with DP-incorporated micelles succeeded in the treatment of rat AMD models, without any sign of side effects, facilitating the development of the DPc-incorporated micelles for cancer photodynamic therapy. Also, the PCI-mediated transfection with gene carriers integrated with DPc allowed the control of transgene expression in the body using light irradiation as an external stimulus. Importantly, the PCI-mediated transfection may not require as high an irradiation energy as PDT, suggesting its potential use for the treatment of deeper tissues, to which PDT is not applicable.

The recent advance in laser technology will allow diverse clinical applications of PDT. For example, the two-photon excitation by using near infrared lasers may have great potential for the PDT of diseases in deeper tissue (*e.g.*, brain tumors). The possibility of two-photon absorption is known to depend linearly on the intrinsic two-photon cross section of the compounds, δ, and quadratically on the incident light intensity.[54] Although the two-photon cross section of molecules is typically small compared with one-photon absorption, neodymium:YAG (Nd:YAG) laser emitting at 1064 nm or tunable solid state lasers generating far-red/near infra-red light could significantly increase the possibility of two-photon absorption of the compounds due to high laser output.[55] In the light of such situations, the development of the delivery systems to improve the biodistribution and enhance the photodynamic efficacy of PSs will be a key technology to effective PDT. Our nanocarriers integrated with dendrimers encapsulating photosensitizers are expected to be a clinically useful PS formulation for PDT and gene therapy.

Acknowledgements

We thank Dr Takuzo Aida, professor in the Department of Chemistry and Biotechnology, Graduate School of Engineering, the University of Tokyo, for valuable discussion on the synthesis of dendrimers encapsulating porphyrins. Also, the authors are grateful to Dr Yasuhiro Tamaki, professor in the Department of Ophthalmology, Graduate School of Medicine, the University of Tokyo, for the accomplishment of the animal experiments. The studies reviewed in this work was supported in part by New Energy and Industrial Technology Development Organization (NEDO) of Japan.

References

1 D. E. J. G. J. Dolmans, D. Fukumura and R. K. Jain, *Nat. Rev. Cancer*, 2003, **3**, 380 387.
2 I. J. Macdonald and T. J. Dougherty, *J. Porphyrins Phthalocyanines*, 2001, **5**, 105 129.
3 R. Z. Renno and J. W. Miller, *Adv. Drug Delivery Rev.*, 2001, **52**, 63 78.
4 M. Tijerina, P. Kopeckova and J. Kopecek, *Photochem. Photobiol.*, 2003, **77**, 645 652.
5 A. S. L. Derycke and P. A. M. de White, *Adv. Drug Delivery Rev.*, 2004, **56**, 17 30.
6 D. Le Garrec, J. Taillefer, J. E. Van Lier, V. Lenaerts and J. C. Leroux, *J. Drug Targeting*, 2002, **10**, 429 437.
7 L. I. Grossweiner, A. S. Patel and J. B. Grossweiner, *Photochem. Photobiol.*, 1982, **36**, 159 167.
8 N. Nishiyama, H. R. Stapert, G. D. Zhang, D. Takasu, D.-L. Jiang, T. Nagano, T. Aida and K. Kataoka, *Bioconjugate Chem.*, 2003, **14**, 58 66.
9 K. Kataoka, A. Harada and Y. Nagasaki, *Adv. Drug Delivery Rev.*, 2001, **47**, 113 131.
10 N. Nishiyama and K. Kataoka, *Adv. Polym. Sci.*, 2006, **193**, 67 101.
11 N. Nishiyama and K. Kataoka, *Pharmacol. Ther.*, 2006, **113**, 630 648.
12 N. Nishiyama, S. Okazaki, H. Cabral, M. Miyamoto, Y. Kato, Y. Sugiyama, K. Nishio, Y. Matsumura and K. Kataoka, *Cancer Res.*, 2003, **63**, 8977 8983.
13 Y. Matsumura and H. Maeda, *Cancer Res.*, 1986, **46**, 6387 6392.
14 R. Ideta, Y. Yanagi, Y. Tamaki, F. Tasaka, A. Harada and K. Kataoka, *FEBS Lett.*, 2004, **557**, 21 25.
15 A. Harada and K. Kataoka, *Science*, 1999, **283**, 65 67.
16 A. Harada and K. Kataoka, *J. Am. Chem. Soc.*, 2003, **125**, 15306 15307.
17 K. Itaka, N. Kanayama, N. Nishiyama, Y. Yamasaki, K. Nakamura, H. Kawaguchi and K. Kataoka, *J. Am. Chem. Soc.*, 2004, **126**, 13612 13613.
18 K. Itaka K, K. Yamauchi, A. Harada, K. Nakamura, H. Kawaguchi and K. Kataoka, *Biomaterials*, 2003, **24**, 4495 4506.
19 H. R. Stapert, N. Nishiyama, D.-L. Jiang, T. Aida and K. Kataoka, *Langmuir*, 2000, **16**, 8182 8188.
20 G.-D. Zhang, A. Harada, N. Nishiyama, D.-L. Jiang, H. Koyama, T. Aida and K. Kataoka, *J. Controlled Release*, 2003, **93**, 141 150.

21 G.-D. Zhang, N. Nishiyama, A. Harada, D.-L. Jiang, T. Aida and K. Kataoka, *Macromolecules*, 2003, **36**, 1304 1309.
22 W.-D. Jang, N. Nishiyama, G.-D. Zhang, A. Harada, D.-L. Jiang, S. Kawauchi, Y. Morimoto, M. Kikuchi, H. Koyama, T. Aida and K. Kataoka, *Angew. Chem.,Int. Ed.*, 2005, **44**, 419 423.
23 S. M. Grayson and J. M. J. Fréchet, *Chem. Rev.*, 2001, **101**, 3819 3867.
24 C. J. Hawker and J. M. J. Fréchet, *J. Am. Chem. Soc.*, 1990, **112**, 7638 7647.
25 R. Sadamoto, N. Tomioka and T. Aida, *J. Am. Chem. Soc.*, 1996, **118**, 3978 3979.
26 C. S. Downes, M. J. Ord, A. M. Mullinger, A. R. Collinsm and R. T. Johnson, *Carcinogenesis*, 1985, **6**, 1343 1352.
27 D. Kessel, Y. Luo, Y. Deng and C. K. Chang, *Photochem. Photobiol.*, 1997, **65**, 422 426.
28 M. Dellinger, *Photochem. Photobiol.*, 1996, **64**, 182 187.
29 K. Berg, P. K. Selbo, L. Prasmickaite, T. E. Tejelle, K. Sandvig, J. Moan, G. Gaudernak, O. Fodstad, S. Kjolsrud, H. Anholt, G. H. Rodal, S. K. Rodal and A. Høgset, *Cancer Res.*, 1999, **59**, 1180 1183.
30 M. R. Hamblin, J. L. Miller, I. Rizvi, B. Ortel, E. V. Maytin and T. Hasan, *Cancer Res.*, 2001, **61**, 7155 7162.
31 S. Sandberg and I. Romslo, *Biochem. J.*, 1981, **198**, 67 74.
32 Y. Kakizawa, A. Harada and K. Kataoka, *J. Am. Chem. Soc.*, 1999, **121**, 11247 11248.
33 I. F. Tannock and D. Rotin, *Cancer Res.*, 1989, **49**, 4373 4384.
34 N. C. Maiti, S. Mazumdar and N. Periasamy, *J. Phys. Chem. B*, 1998, **102**, 1528 1538.
35 K. M. Kadish, G. B. Maiya, C. Araullo and R. Guilard, *Inorg. Chem.*, 1989, **28**, 2725 2731.
36 R. Savic, L. Luo, A. Eisenberg and D. Maysinger, *Science*, 2003, **300**, 615 618.
37 TAP and VIP Study Group, *Retina*, 2002, **22**, 6 18.
38 R. Ideta, F. Tasaka, W.-D. Jang, N. Nishiyama, G.-D. Zhang, A. Harada, Y. Yanagi, Y. Tamaki, T. Aida and K. Kataoka, *Nano Lett.*, 2005, **5**, 2426 2431.
39 D. N. Zacks, E. Ezra, Y. Terada, N. Micband, E. Connolly, E. S. Gragoudas and J. W. Miller, *Invest. Ophthalmol. Visual Sci.*, 2002, **43**, 2384 2391.
40 J. Moan and K. Berg, *Int. J. Cancer*, 1994, **58**, 865 870.
41 A. C. H. Ng, X. Li and D. K. P. Ng, *Macromolecules*, 1999, **32**, 5292 5298.
42 W.-D. Jang, Y. Nakagishi, N. Nishiyama, S. Kawauchi, Y. Morimoto, M. Kikuchi and K. Kataoka, *J. Controlled Release*, 2006, **113**, 73 79.
43 A. Høgset, L. Prasmickaite, T. E. Tejelle and K. Berg, *Hum. Gene Ther.*, 2000, **11**, 869 880.
44 L. Prasmickaite, A. Høgset and K. Berg, *Photochem. Photobiol.*, 2001, **73**, 388 395.
45 A. Høgset, L. Prasmickaite, M. Hellum, B. Æ. Engesæter, V. M. Olsen, T. Tejelle, C. J. Wheeler and K. Berg, *Somatic Cell Mol. Genet.*, 2002, **27**, 97 113.
46 A. Høgset, L. Prasmickaite, P. K. Selbo, M. Hellum, B. Æ. Engesæter, A. Bondted and K. Berg, *Adv. Drug Delivery Rev.*, 2004, **56**, 95 115.
47 N. Nishiyama, Arnida, W.-D. Jang, K. Date, K. Miyata and K. Kataoka, *J. Drug Targeting*, 2006, **14**, 413 424.
48 Arnida, N. Nishiyama, N. Kanayama, W.-D. Jang, Y. Yamasaki and K. Kataoka, *J. Controlled Release*, 2006, **115**, 208 215.
49 O. Boussif, F. Lezoualc'h, M. A. Zanta, M. D. Mergny, D. Scherman, B. Demeneix and J. P. Behr, *Proc. Natl. Acad. Sci. U. S. A.*, 1995, **92**, 7297 7301.
50 N. Nishiyama, A. Iriyama, W.-D. Jang, K. Miyata, K. Itaka, Y. Inoue, H. Takahashi, Y. Yanagi, H. Koyama and K. Kataoka, *Nat. Mater.*, 2005, **4**, 934 941.
51 F. Caruso, R. A. Caruso and H. Möhwald, *Science*, 1998, **282**, 1111 1114.
52 E. Donath, G. B. Sukhorukov, F. Caruso, S. A. Davis and H. Möhwald, *Angew. Chem., Int. Ed.*, 1998, **37**, 2201 2205.
53 C. Rudolph, C. Plank, J. Lausier, U. Schillinger, R. H. Muller and J. Rosenecker, *J. Biol. Chem.*, 2003, **278**, 11411 11418.
54 D. H. Oh, R. J. Stanley, M. Lin, W. K. Hoeffler, S. G. Boxer, M. W. Berns and E. Bauer, *Photochem. Photobiol.*, 1997, **65**, 91 95.
55 A. M. R. Fisher, A. L. Murphree and C. J. Gomer, *Lasers Surg. Med.*, 1995, **17**, 2 31.

